Theoret. chim. Acta (Berl.) 6, 363—400 (1966)

Commentationes

Porphyrins

VIII. Extended Hückel Calculations on Iron Complexes

MICHAEL ZERNER*, MARTIN GOUTERMAN, and HIROSHI KOBAYASHI

Conant Chemical Laboratory, Harvard University, Cambridge, Massachusetts 02138

Received July 5, 1966

The extended Hückel model is further developed to allow prediction of spin state and is applied to ferrous porphin complexes with H_2O, CO, O_2, N_2 and ferric porphin complexes with OH^-, F^-, Cl^-, CN^-. The model shows that if the iron atom lies in the porphyrin plane only low or intermediate spin states are possible, with the weakest ligands just producing low spin. The high spin ("ionic") complex can only occur with iron displaced from the plane, in which geometry CO and CN^- are calculated to be low spin, OH^-, F^-, Cl^- high spin, and H_2O borderline between low and high. The model predicts that N_2 will not bond and that a stable O_2 complex is impossible if O_2 is perpendicular to the plane. Discussion is given of the ligand field, absorption spectra, soft X-ray spectra, and Mössbauer spectra.

Le modèle de Hückel étendu est élaboré de manière á permettre la prédiction de l'état de spin et est appliqué aux complexes de la porphine ferreuse avec H_2O, CO, O_2, N_2 et de la porphine ferrique avec OH^-, F^-, Cl^-, CN^-. Ce modèle montre que, si l'atome de fer se trouve dans le plan de la porphyrine, seuls des états de spin bas et intermédiaires sont possibles, les ligands les plus faibles donnant seulement un spin bas. Le complexe à spin élevé (ionique) ne peut exister qu'avec le fer en dehors du plan, auquel cas on calcule un spin bas pour CO et CN^-, haut pour OH^-, F^-, Cl^-, et l'un ou l'autre pour H_2O. Ce modèle permet de prédire que N_2 ne se liera pas et qu'un complexe stable avec O_2 est impossible si O_2 est perpendiculaire au plan. On discute le champ des ligands, le spectre d'absorption, le spectre des rayons X mous et le spectre Mössbauer.

Das erweiterte Hückelmodell wird in einer Weise ausgebaut, daß Aussagen über Spinzustände möglich werden. Das Verfahren wird auf eisen-(II)-haltige Porphyrinkomplexe mit H_2O, CO, O_2 und N_2 als Liganden und eisen-(III)-haltige Komplexe mit OH^-, F^-, Cl^- und CN^- angewendet. Dabei zeigt sich, daß nur Zustände mit niedrigem oder mittlerem Spin möglich sind, wenn das Eisenatom in der Porphyrin-Ebene liegt, und daß dabei die schwächsten Liganden den niedrigsten Spin ergeben. Komplexe mit hohem Spin („Ionenkomplexe") sind nur dann möglich, wenn das Eisen nicht in der Ebene liegt, und zwar haben dann der CO- und der CN^--Komplex niedrigen, der OH^--, F^-- und Cl^--Komplex hohen und der H_2O-Komplex entweder hohen oder niedrigen Spin. Das Modell ergibt ferner, daß N_2 nicht gebunden wird und daß ein stabiler O_2-Komplex nur entsteht, wenn das O_2-Molekül senkrecht zur Bindungsebene steht. Zum Schluß werden Ligandenfeld, Absorptionsspektren, weiche Röntgenspektren und Mössbauerspektren diskutiert.

This paper is part of a series on the electronic theory and spectra of porphyrins. The first three papers were concerned with the π electrons. Paper I presented experimental facts on porphyrin spectra and offered simple quantum mechanical

* National Institutes of Health Pre-Doctoral Fellow.

models of a free electron nature [*26*]. Paper II attempted to refine the models to quantitative accuracy [*27*]. Finally, Paper III applied to the porphyrin π electrons self-consistent molecular orbital (SCMO) theory using the method of Pariser, Parr, and Pople (PPP) for evaluating integrals [*74*]. This model was reasonably successful in accounting for the π electron spectra.

With Paper IV a new series was begun which applied extended Hückel (EH) theory to all the electrons of porphyrin with particular emphasis on the ligand field of the transition metal complex [*77*]. The model used a self-consistent charge (SCC) refinement. Paper IV applied the model to complexes of the transition metals Mn through Zn. Paper V [*78*] considered VO and V complexes, exploring the problem of metal non-planarity, the EPR data on the VO complex, and the apparent chemical instability of the V complex. Paper VI [*78*] considered the hypothetical ScOH complex. (Paper VII [*17*] presents experimental vapor phase spectra.)

The iron complexes, which because of their biological activity have been extensively investigated experimentally and are of great general interest, were only given cursory examination in Paper IV, which reported on the planar ferrous complex without fifth and sixth ligands. The present paper reports an extensive set of SCC–EH calculations on ferrous and ferric porphins and their common complexes, and relates the theoretical results to various spectroscopic, magnetic, and chemical facts.

Previous calculations employing the Wolfsberg-Helmholtz Hamiltonian which underlies the extended Hückel method have been made on iron porphyrins by Pullman, Berthier and Spanjaard [*62*] as well as Ohno, Tanabe and Sasaki [*55*], but these calculations made use of a limited basis set including only the π electron orbitals, sp^2 hybrids on the neighboring nitrogen atoms of porphin, and the $3d$, $4s$, $4p$ orbitals of Fe. More recently Berthier, Millie and Veillard [*4*] investigated the environment of the central iron using a somewhat more sophisticated Hamiltonian. Because of the restricted basis set used, these calculations attempt to relate only to limited data. The present SCC–EH calculations include explicitly all the valence orbitals of all atoms in the molecular complex and should not only reflect the properties of the central Fe but also those inherent to porphyrin and to any additional fifth and sixth ligands.

The limitations of the extended Hückel model were discussed at some length previously [*77*], and we have not forgotten them. We caution the reader to do likewise.

Method

a) General

The extended Hückel (EH) model with self-sonsistent charge (SCC) was presented before, and we here merely recapitulate what was said earlier [*77*]. We seek solutions to the molecular equation

$$H_{\text{eff}}\,\phi_j = w_j\,\phi_j$$

where the molecular orbitals ϕ_j are expanded in terms of Slater atomic orbitals

$$\chi(n, l, m) = N r^{n-l} \exp(-\zeta r)\; Y_l^m(\theta, \phi)\,.$$

Table 1. H_{pp}(eV)[a]

	$A^- \rightarrow A + (e)$	$A \rightarrow A^+ + (e)$	$A^+ \rightarrow A^{+2} + (e)$
O[b]	$s^2x^2y^2z \rightarrow sx^2y^2z + (s) - 19.240$	$s^2x^2yz \rightarrow sx^2yz + (s) - 32.367$	$s^2xyz \rightarrow sxyz + (s) - 47.84$
	$s^2x^2y^2z \rightarrow s^2x^2yz + (p) - 1.934$	$s^2x^2yz \rightarrow s^2xyz + (p) - 15.863$	$s^2xyz \rightarrow s^2xy + (p) - 33.63$
Cl[c]	$s^2x^2y^2z \rightarrow sx^2y^2z^2 + (s) - 14.46$	$s^2x^2y^2z \rightarrow sx^2y^2z + (s) - 24.02$	
	$s^2x^2y^2z \rightarrow s^2x^2y^2z + (p) - 3.74$	$s^2x^2y^2z \rightarrow s^2x^2yz + (p) - 15.03$	

[a] See also Tabs. 5 and 6, Paper IV, [77]; the value given for Fe as 8.70 should be 8.77.

[b] From PILCHER, G., and H. A. SKINNER: J. Inorg. Nucl. Chem. **24**, 937 (1962).

[c] Estimated from the atomic spectral tables of C. E. MOORE: Atomic energy levels, (Nat. Bu Stands., Washington, Circular 467 (1948)), Vol. 1, using the methods described in b. above. Since tl chlorine atom is never calculated to have a net positive charge, ionization potentials for $Cl^+ \rightarrow Cl^{+2} + (e)$ are never needed.

The calculation makes use of all valence orbitals of each atom; i.e., (1*s*), (2*s*, 2*p*), (3*s*, 3*p*), or (3*d*, 4*s*, 4*p*), as appropriate. The expansion is carried out as

$$\phi_j = \sum_p \chi_p \, c_{pj} \, .$$

The coefficients c_{pj} and energies w_j are determined in the usual manner [58] from the overlap integrals $S_{pq} = \langle \chi_p \mid \chi_q \rangle$ and the Hamiltonian integrals. The latter are approximated by what is sometimes called the Wolfsberg-Helmholtz Hamiltonian [52, 75]

$$\langle \chi_p \mid H_{\text{eff}} \mid \chi_q \rangle \equiv H_{pq} = \tfrac{1}{2} (H_{pp} + H_{qq}) \, S_{pq} \, [\varkappa + (1 - \varkappa) \, \delta_{pq}] \, ,$$

where H_{pp} are related to atomic valence state ionization potentials. The SCC refinement [77] first determines c_{pj} from the values for neutral atoms, H^0_{pp}, then readjusts H_{pp} between neutral and ionic values, $H^{\pm}_{pp}$, based on the charge calculated for atom p by a Mulliken population analysis [53]. Iterations are continued until calculated and assumed charges agree within 0.05 electrons [77]. The procedure resembles that of the self-consistent field [64].

Table 2. *Basis Set Exponentials*[a] *(Bohr radii)*$^{-1}$

	s	*p*
O	2.2458	2.2266
Cl	2.3561	2.0387

[a] From [12]. See also Tab. 3, Paper IV, [4].

The energies w_j and coefficients c_{pj} are therefore fully determined by the neutral and ionic energies, H^0_{pp} and $H^{\pm}_{pp}$, the orbital exponents ζ_p, and the interaction parameter $\varkappa$. The present calculations make use of the same values for the energies and exponents of the atomic orbitals on H, C, N, Fe as were given in Paper IV, Tabs. 3, 5, and 6. The necessary values for O and Cl, which are needed for the present paper, are given in Tabs. 1 and 2.

As discussed previously, the exponents for C and N were taken from CLEMENTI and RAIMONDI [10], who determined the best single exponents by variational calculations. These values were also used for O and Cl. However, for Fe the best single exponential functions were not in good agreement with accurate Hartree-Fock 3*d* orbitals [11] and were particularly bad for calculating iron-nitrogen overlap integrals. We therefore used for 3*d* orbitals a single ζ which best reproduced the overlaps between the accurate 3*d* functions of WATSON [73] and the best single exponential nitrogen orbitals. For iron a single ζ reproduces all the resulting

overlaps of the Watson $3d$ functions (d^6s^2) and the nitrogen orbitals at the distance present in an average porphyrin (2.054 Å) within ~5%. The next-nearest neighbor overlaps are all underestimated by about 25%; but, as the non-nearest neighbor overlaps are much smaller, this error proves not to be very important in determining the ligand field. The only important error, then, could stem from the additional complexing ligands added above and below the porphin plane, about the central iron atom. The chelating atoms of these additional ligands, however, fall within 1.84 Å to 2.09 Å of the iron atom, near the 2.054 Å interatomic distance for which the functions were fit, and the error is small. For the other atoms of the ligand groups, further from the central iron, the overlap is small.

The $4s$ exponential constant was fitted to the many term Watson $4s$ orbitals in a similar manner to that employed for the $3d$. In this case the exponent derived is very similar to that obtained by the variational calculations of CLEMENTI and RAIMONDI [*10*] assuming a single exponential function. No sizable error in overlap results using this single value. The $4p$ exponent is set equal to that of the $4s$ for reasons detailed in Paper IV.

We have used in the present calculations $\varkappa = 1.89$, the value used in all our previous SCC–EH calculations. This value is derived to fit the average singlet and triplet energy of the two lowest $\pi \rightarrow \pi^*$ excitations,

$$a_{2u}(\pi) \rightarrow e_g^*(\pi) \text{ and } a_{1u}(\pi) \rightarrow e_g^*(\pi) .$$

As discussed in previous work on the π electrons [*26*, *27*, *74*], the singlets of these transitions are subject to extensive configuration interaction; hence this averaging seems appropriate. In obtaining the average we used the two lowest observed singlets of tetraphenylporphin, the lowest observed triplet, of mesoporphyrin [*3*] (corrected to correspond to tetraphenylporphin), and a second triplet estimated to be 0.1 eV above the first from SCMO–PPP calculations [*74*].

Two further points might be mentioned. In cases where the electron assignment incompletely filled a degenerate pair of orbitals, for the SCC calculation a symmetrized charge distribution was used. Thus for $e_g(d_{xz})^2 e_g(d_{yz})$ we used $e_g(d_{xz})^{3/2}$ $e_g(d_{yz})^{3/2}$. Reasons for adopting this procedure have been given [*77*].

A second point is that in some high spin calculations we have placed an unpaired electron in an orbital $b_{1g}(d_{x^2-y^2})$, even though the empty $e_g^*(\pi)$ orbitals of porphin appear to have lower energy. This is necessary, for if the electron were placed in $e_g^*(\pi)$ all metal orbitals would be greatly lowered in energy through the SCC procedure. Not only would $b_{1g}(d_{x^2-y^2})$ now have lower energy than $e_g^*(\pi)$, but the partially filled $e_g(d_\pi)$ and $a_{1g}(d_{z^2})$ would now be below the filled porphin MO $a_{2u}(\pi)$, presenting a completely unreasonable picture.

b) Development of a Spin Model

As is well known from atomic spectroscopy, a given electronic configuration gives rise to a number of distinct terms. These terms have orbital degeneracy $2L + 1$ and spin degeneracy $2S + 1$. A one electron model determines orbital energies $w(j)$. Differences between these should correspond to differences in energy between electronic configurations, i.e., some type of average among the term energies that arise from a configuration. However, it is important to determine individual term energies, particularly for the present problem, because the self-

consistent charge procedure demands knowledge of the ground configuration. Because splitting among terms is large, the ground configuration is often not obtained by spin pairing electrons in MO's in order of increasing energy. Thus before electrons can be assigned and the self consistent charge procedure performed, the relative energies of low lying terms must be determined.

We use for configuration energy the average of the energy of each term weighted by its orbital degeneracy only. An alternative procedure would weight each term by its spin multiplicity as well. We call the first the *term average* energy while the second is the average energy. In the framework of a spinless model it is difficult to choose between various methods of averaging term energies. However, the interaction parameter $\varkappa$ was determined by averaging the experimental singlet and triplet $\pi \rightarrow \pi^*$ transition energies without spin weighting the triplet [77]. For this reason we have proceeded by assuming that energy differences $w(j) - w(i)$ correspond to differences in configuration energy, the latter based on the term average. Individual term energies are determined by adding in the exchange integrals that cause the term energy to differ from this average. Consistent use of the spin weighted average energy has proven to give very similar numerical results.

We here examine low lying d^6 (ferrous) and d^5 (ferric) configurations arising from a square planar, or nearly square planar, ligand field (D_{4h}). The shorthand notation used is

$$a = b_{2g}(d_{xy}),\ b = e_g(d_{yz}),\ c = e_g(d_{xz}),\ d = a_{1g}(d_{z^2}),\ e = b_{1g}(d_{x^2-y^2}).$$

The low lying orbitals for d^6 are shown in the following schematic diagram:

	d^6	
$-e$	$-$	$+$
$-d$	$+$	$+$
$+c\ +b$	$+\ +$	$+\ +$
$+a$	$+$	$+$
"A"	"B"	"D"
$^1A_{1g}$	$^3E_g, {}^1E_g$	$^5B_{2g}, {}^3A_{2g}, {}^3B'_{2g}$ $^3B''_{2g}, {}^1A_{2g}, {}^1B'_{2g}$.

The wave functions arising from such configurations appear elsewhere [76]. The average term energies are:

$$\overline{E}_A = {}^1E_A = W_A$$
$$\overline{E}_B = W_B$$
$$\overline{E}_D = W_D - \tfrac{1}{3}(K_{bc} + K_{bd} + K_{be} + K_{cd} + K_{ce} + K_{de}).$$

Here the W_k's are the one and two electron terms which all the spin states arising from a given configuration have in common. By assumption their explicit form will not be needed. In terms of the solutions of the SCC–EH model, according to our model,

$$\overline{E}_B - \overline{E}_A = W_B - W_A \approx w(d) - w(c)$$
$$\overline{E}_D - \overline{E}_A = W_D - \tfrac{1}{3}(K_{bc} + K_{bd} + K_{be} + K_{cd} + K_{ce} + K_{de}) - W_A$$
$$\approx w(d) + w(e) - w(b) - w(c).$$

Differences in energy between low lying states are thus:

$$^3E_B - {}^1E_A \approx w(d) - w(c) - K_{cd}$$

$$^5E_D - {}^1E_A \approx w(e) + w(d) - w(b) - w(c) - \tfrac{2}{3}(K_{bc} + K_{bd} + K_{be} + K_{cd} + K_{ce} + K_{de})$$

$$^5E_D - {}^3E_B \approx w(e) - w(b) - \tfrac{2}{3}(K_{bc} + K_{bd} + K_{be} + K_{ce} + K_{de}) + \tfrac{1}{3} K_{cd}\,.$$

Similarly for d^5 a schematic for the low lying configurations is:

		d^5	
$-e$	$-$	$-$	$+$
$-d$	$+$	$+$	$+$
$+c \;+\!+\; b$	$+\;+$	$-\;+\!+$	$+\;+$
$+\!+a$	$+\!+$	$+\!+$	$+$
"A"	"B"	"C"	"D"
^2E_g	$^4A_{2g}, {}^2B_{2g}, {}^2A'_{2g}$	$^2A_{1g}, {}^2B'_{1g}$	$^6A_{1g}, {}^4A_{1g}, {}^4A'_{1g}, {}^4A''_{1g}, {}^4B'''_{1g}$ $^2A_{1g}, {}^2A'_{1g}, {}^2A''_{2g}, {}^2B'''_{1g}, {}^2B''''_{1g}$

$$\overline{E}_A = {}^2E_A = W_A$$

$$\overline{E}_B = W_B - \tfrac{1}{3}(K_{cd} + K_{bd} + K_{bc})$$

$$\overline{E}_C = W_C - \tfrac{1}{2}(K_{bd} + K_{bc})$$

$$\overline{E}_D = W_D - \tfrac{2}{5}(K_{ab} + K_{ac} + K_{ad} + K_{ae} + K_{bc} + K_{bd} + K_{be} + K_{cd} + K_{ce} + K_{de}).$$

Configurations "B" and "C" have been considered independently, as W_B and W_C differ by coulomb integrals;

$$W_C - W_B = \tfrac{1}{2}(J_{bb} + J_{cc}) - J_{bc} = 2K_{bc}^{\star}\,.$$

Results most consistent with experiment are obtained if we set

$$\overline{E}_B - \overline{E}_A \equiv w(d) - w(b)$$

and

$$\overline{E}_C - \overline{E}_A \equiv w(d) - w(b) + 2K_{bc}\,.$$

Differences between states of suspected low lying energy are thus given by:

$$^4E_B - {}^2E_A \approx w(d) - w(b) - \tfrac{2}{3}(K_{bd} + K_{cd} + K_{bc})$$

$$^6E_D - {}^2E_A \approx w(d) + w(e) - w(a) - w(b) - \tfrac{3}{5}(K_{ab} + K_{ac} + K_{ad} + K_{ae} + K_{bc} + K_{bd} + K_{be} + K_{cd} + K_{ce} + K_{de})\,.$$

In this we use the notation ^4E_B, ^2E_B, $^2E'_B$ to refer to states $^4A_{1g}$, $^2B_{2g}$, $^2A'_{2g}$ derived from configuration "B".

We now turn our attention to an evaluation of the exchange integrals which, when combined with the computed MO energies $w(i)$ from the SCC–EH method, should give us an estimate of ligand field transition energies and indicate the lowest energy state of a transition metal complex.

In an almost identical manner to that applied to derive the energy of different ligand field states in terms of exchange and repulsion integrals, the energy of the various different atomic terms of the transition metals can be evaluated. This has

* This can be readily shown from expansion of the Coulomb and exchange integrals in terms of Slater-Condon factors in a manner similar to that to be described. See also [76].

been performed by various authors for many electronic configuration [*12, 69, 63*]. The analytic expressions for the Coulomb and exchange integrals are formalized in terms of the Slater-Condon integrals, F, ("factors") resulting from an expansion of $1/r_{ij}$ and re-expression of these integrals as combinations of new integrals over spherical harmonics. These "factors" can then be evaluated from atomic-spectra.

With these atomic parameters at hand from previous investigations [*35, 68*] it is now necessary to evaluate the exchange integrals between cubic field d orbitals in terms of the Slater-Condon factors. This is done by re-expressing the cubic field orbitals in terms of their angular momentum components. This leads to [*76*]:

$$\begin{aligned} K(xy, yz) = K(xy, xz) = K(xz, yz) = K(x^2 - y^2, xz) = K(x^2 - y^2, yz) \\ = 3F_2 + 20F_4 = 0.631, 0.781 \text{ eV} \\ K(z^2, x^2 - y^2) = K(z^2, xy) = 4F_2 + 15F_4 = 0.731, 0.878 \text{ eV} \\ K(z^2, xz) = K(z^2, yz) = F_2 + 30F_4 = 0.430, 0.587 \text{ eV} \\ K(x^2 - y^2, xy) = 35F_4 = 0.330, 0.490 \text{ eV} . \end{aligned}$$

The numbers which appear in these expressions were obtained using the Slater-Condon factors worked out by HINZE and JAFFÉ [*35*]; the first value is for neutral iron, the second, for the cation. Since the Slater-Condon factors are charge dependent, we extrapolate between the neutral and appropriate ionic value.

For an average net charge on Fe of about $+0.20$, we get for d^6 transitions:

$$\begin{aligned} {}^3E_B - {}^1E_A &\approx w(d) - w(b) - 0.46 \text{ eV} \\ {}^5E_D - {}^1E_A &\approx w(e) + w(d) - w(b) - w(c) - 2.44 \text{ eV} \\ {}^5E_D - {}^3E_B &\approx w(e) - w(c) - 1.98 \text{ eV} . \end{aligned}$$

For d^5:

$$\begin{aligned} {}^4E_B - {}^2E_A &\approx w(d) - w(b) - 1.06 \text{ eV} \\ {}^6E_D - {}^2E_A &\approx w(d) + w(e) - w(a) - w(b) - 3.73 \text{ eV} \\ {}^6E_D - {}^4E_B &\approx w(e) - w(a) - 2.67 \text{ eV} . \end{aligned}$$

The above scheme of incorporating two electron terms obtained empirically from atomic parameters into the essentially one electron extended Hückel calculations rest heavily upon the fact that the ligand field orbitals of transition elements are essentially atomic orbitals. This, from experience with the model and from information from many EPR experiments, is often the case. The application of this method to highly perturbed metal orbitals (and thus heavy mixing of the metal d functions with the ligand orbitals) must be done with full recognition that the two electron terms are being incorrectly estimated for our purposes.

One point should be stressed and remembered throughout the ensuing discussions. We fit the $\pi \rightarrow \pi^*$ excitations with a single $\varkappa$. The resulting energy levels may therefore not accurately predict $d \rightarrow d$, $n \rightarrow \pi^*$, and charge transfer transitions.

c) Geometric Considerations

Although it has been found that the tetradentate porphin molecule is seldom planar [*36, 20, 67*], it was shown that these slight non-planarities little affect the

results of these calculations (Paper IV). We thus use a planar projection of the X-ray coordinates of HOARD, HAMOR and HAMOR [*36*] in which we have paid special attention to the preservation of the observed bond lengths. These coordinates, presented in Fig. 1 and in Tab. 3, are the same used for all previous porphin calculations of this series, and are therefore a constant of these calculations; the *exceptions* are the locations of the four nitrogen atoms [*77*], which for most of these iron calculations are radially displaced to a position 2.03 Å from the porphin center as suggested by the X-ray studies on ferric porphyrins by FLEISCHER, MILLER and WEBB [*20*] and HOARD, HAMOR, HAMOR and CAUGHEY [*37*].

There is some debate on how far the Fe(III) atom is above the plane of the four neighboring nitrogens of porphin. Estimates range from 0.20 Å to 0.475 Å [*20, 37, 42*]. We choose the value 0.455 Å for Fe(III) and use it for all spin cases, although it has been suggested that low spin Fe(III) might lie in the nitrogen plane [*37*]. The uncertainty in the position of low spin Fe(III) in these molecular systems does not greatly influence these results, affecting mainly the location of the $3d_{x^2-y^2}$ ligand field orbital; that is, the more nearly planar the system, the higher in energy is this orbital. Since the only low spin ferric complex we examine, that of CN^-, is predicted low spin at the elevated geometry, it would certainly be low spin in the more planar situation. As this "troublesome" orbital is unoccupied in either case it has very little influence on the charge field set up by the self-consistent charge procedure.

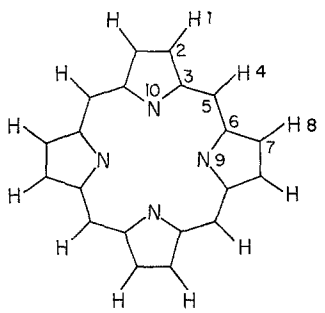

Fig. 1. Geometry and Labeling of Planar Porphin

Table 3. *Coordinates (x,y,z) of Porphin in Angstroms*[a]

H(1)	1.325, 5.084, 0.0
C(2)	0.681, 4.217, 0.0
C(3)	1.098, 2.839, 0.0
H(4)	3.208, 3.208, 0.0
C(5)	2.444, 2.444, 0.0
C(6)	2.839, 1.098, 0.0
C(7)	4.217, 0.681, 0.0
H(8)	5.084, 1.325, 0.0
N(9)[b]	2.054, 0.000, 0.0
N(10)[b]	0.000, 2.054, 0.0

[a] Planar projection of tetraphenyl porphyrins [*36*] with special attention paid to preserving bond lengths. C–H bonds set at 1.08 Å.

[b] These nitrogens are radially displaced in a manner appropriate to each central environment; for the iron calculations presented here, the nitrogens are placed at 2.03 Å from the porphin center, see text.

The Fe(II) compounds have been investigated in somewhat greater detail, some being considered planar, others with the Fe(II) atom 0,492 Å above the plane. Although myoglobin studies give a smaller displacement [*41*], the uncertanties in the protein studies are quite large. The elevation of 0.492 Å is suggested by an investigation of the bond lengths of ferrous and ferric compounds, and a comparison with the observed ferric coordinates of Ref. [*37*]. The nitrogen positions, at 2.03 Å from the porphin center, are preserved, although one might move

Table 4. *Coordinates (x,y,z) of* Fe *Porphin Complexes in Angstroms*

Case	Complex	Coordinates
I	Fe(II), $S = 1$ D_{4h}	Fe(0.0,0.0,0.0)
II	Fe(II), $S = 1$ C_{4v}	Fe(0.0,0.0,0.492)
III	Fe(II), $S = 2$ C_{4v}	Fe(0.0,0.0,0.492)
IV[a]	Fe(II) – 5 – H_2O, $S = 0$ C_{2v}	Fe(0.0,0.0,0.0), O(0.0,0.0,2.09), H(0.0,0.800,2.618)
V[a]	Fe(II) – 5 – H_2O, $S = 0$ C_{2v}	Fe(0.0,0.0,0.492), O(0.0,0.0,2.582), H(0.0,0.800,3.110)
VI[a]	Fe(II) – 5 – H_2O, $S = 2$ C_{2v}	Fe(0.0,0.0,0.492), O(0.0,0.0,2.582), H(0.0,0.800,3.110)
VII[a]	Fe(II) – 5, 6 – $(H_2O)_2$, $S = 0$ S_4	Fe(0.0,0.0,0.0,) O(0.0,0.0,2.09), H(0.800,0.0,2.618) O(0.0,0.0, –2.090), H(0.0,0.800, –2.618)
VIII[a]	Fe(II) – 5, 6 – $(H_2O)_2$, $S = 0$ C_{2v}	Fe(0.0,0.0,0.492), O(0.0,0.0,2.582), H(0.800,0.0,3.110) O(0.0,0.0, –2.09), H(0.0,0.800, –2.618)
IX[b]	Fe(III) – 5 – CN, $S = \frac{1}{2}$ C_{4v}	Fe(0.0,0.0,0.455), C(0.0,0.0,2.295), N(0.0,0.0,3.452)
X[c]	Fe(III) – 5 – Cl, $S = \frac{5}{2}$ C_{4v}	Fe(0.0,0.0,0.455), Cl(0.0,0.0,2.670)
XI[d]	Fe(III) – 5 – OH, $S = \frac{5}{2}$ C_{4v}	Fe(0.0,0.0,0.455), O(0.0,0.0,2.297), H(0.0,0.0,3.281)
XII[e]	Fe(II) – 5 – CO, $S = 0$ C_{4v}	Fe(0.0,0.0,0.492), O(0.0,0.0,3.462), C(0.0,0.0,2.332)
XIII[f]	Fe(II) – 5 – O_2 – 6 – H_2O, $S = 0$ C_{2v} (coplanar)	Fe(0.0,0.0,0.492), O(0.0,0.0, –2.09), H(0.0,0.800, –2.618), O(0.608,0.0,2.01)
XIV[f]	Fe(II) – 5 – O_2 – 6 – H_2O, $S = 1$ C_{2v} (coaxial)	Fe(0.0,0.0,0.492), O(0.0,0.0, –2.09), H(0.0,0.800, –2.618), O(0.0,0.0,2.582), O(0.0,0.0,3.798)
XV[g]	Fe(II) – 5 – N_2, $S = 0$ C_{2v} (coplanar)	Fe(0.0,0.0,0.492), N(0.547,0.0,2.498)
XVI[g]	Fe(II) – 5 – N_2, $S = 0$ C_{4v} (coaxial)	Fe(0.0,0.0,0.492), N(0.0,0.0,2.592), N(0.0,0.0,3.686)

[a] Fe–O set at 2.09 Å from $FeCl_2 \cdot 4H_2O$, from [*59*]; coordinates of H_2O from footnote [h] below.

[b] Fe–C set at 1.84 Å from $Fe(CNCH_3)_6 Cl_2 \cdot 3H_2O$, [*61*]; C≡N, 1.157 Å from average X–Cl footnote [h] below.

[c] Fe–Cl set at 2.218 from haemin, [*42*].

[d] Fe–OH 1.842 Å from methoxyferrous mesoporphyrin IX dimethyl ester, [*37*], although th may be somewhat short; O–H, 0.984 Å from average X–OH, footnote [h], below.

[e] Fe–C set at 1.84 Å from $Fe(NO_2)_2 \cdot 2CO$, [*7*]; C≡O, 1.13 Å from CO, [*34*].

[f] Fe–O set at 2.1 Å from covalent radii, and [*59*]; O–O, 1.216 Å in O_2, [*34*].

[g] Fe–N distance set at 2.1 Å from covalent radii; N–N, 1.094 Å in N_2, [*34*].

[h] Tables of interatomic distances and configurations in molecules and ions [The Chemic Society, London, Special publications **11** (1958), **18** (1965)].

the nitrogen atoms out as far as 2.06 Å, the maximum suggested from the stericly crowded free base [*36, 67*], allowing the Fe(II) atom to come more into the porphin plane.

The geometries used for the present calculations are given in Tab. 4.

Results

In the following discussion we generally use D_{4h} nomenclature for labeling orbitals even though the nonplanarity of the iron and the extra ligands sometimes reduce the symmetry to C_{4v} or C_{2v}. For orbitals that have no analogue in the D_{4h} case and for cases where the symmetry has been severely affected by ligands we use the C_{2v} names, as our computer programs demanded at least this symmetry. The following correspondence exists between the two sets of labels:

$$e_g,\ e_u \to b_1,\ b_2;\ a_{1g},\ b_{1g},\ a_{2u},\ b_{2u} \to a_1;\ a_{1u},\ b_{1u},\ a_{2g},\ b_{2g} \to a_2\ .$$

a) Ferrous Porphin and Ferrous Porphin Hydrates (Cases I to VIII).

Ferrous porphin and complexes of ferrous porphin with water establish the same ligand field order that we have calculated for all previous transition metal porphins [*77*]. In order of increasing energy these orbitals are

$$b_{2g}(d_{xy}) \lesssim e_g(d_\pi) \lesssim a_{1g}(d_{z^2}) < b_{1g}(d_{x^2-y^2})\ .$$

The changes caused by raising the iron atom out of the porphin plane and by addition of fifth and sixth water molecules affects the various orbital energy gaps, and particularly the energy of the $a_{1g}(d_{z^2})$, but the order of orbitals is unchanged.

Planar Fe(II) porphin (Case I), using the criterion established in the previous section, is predicted to be of "intermediate" spin, ^3E_g.

$$(b_{2g})^2\ (e_g)^3\ (a_{1g})^1\ .$$

Although this appears to be the situation in Fe(II) phthalocyanines from magnetic susceptibility studies [*47*], it may be the only spin state not available to Fe(II) porphyrins [*22, 28*]. However, the iron atom in Fe(II) phthalocyanine may be in the molecular plane* while that of Fe(II) porphin has been shown out of plane. A subsequent calculation with Fe(II) raised 0.492 Å out of the porphin plane (Cases II and III) indicates high spin, $^5B_{2g}$.

$$(b_{2g})^2\ (e_g)^2\ (a_{1g})^1\ (b_{1g})^1\ .$$

The increased spin obtained is a result of the greatly reduced energy of the $b_{1g}(d_{x^2-y^2})$ ligand field orbital, no longer pointing directly into the porphin nitrogen atoms. Correspondingly, the other ligand field orbitals are somewhat raised in an apparent attempt to preserve the center of gravity, further reducing the *d-d* energy gaps. Any further increase in non-planarity indicates high spin, any increase in planarity, intermediate spin. These results are demonstrated in Fig. 2.

Placement of a water molecule 2.1 Å above the iron atom in planar Fe(II) porphin (Case IV) produces a low spin situation by raising the $a_{1g}(d_{z^2})$ ligand field orbital, as shown in Fig. 2. However, in the case of non-planar Fe(II) porphin the addition of a single water molecule produces either a spin of 0 or 2 but not 1. The energy gap between the low energy $b_{2g}(d_{xy})$ and the high energy $b_{1g}(d_{x^2-y^2})$ is sufficiently small with non-planar iron that as the $a_{1g}(d_{z^2})$ orbital rises in energy the system goes directly from high spin to low spin. However, the balance is very

* The lone pair electrons associated with the four bridge nitrogen atoms may produce extra bonding of the iron to phthalocyanine as compared to porphyrin. This may be the cause of the known shorter metal nitrogen bonds [*30*] and may keep the iron in-plane.

delicate. A calculation on this system assuming low spin produces a ligand field manifold suggesting high spin; a calculation assuming high spin produces orbitals indicating low spin. For the non-planar Fe(II) monohydrate complexes (Cases V and VI), the $b_{2g}(d_{xy})$ orbital lies between 400 and 800 cm^{-1} below the lowest $e_g(d_\pi)$. The degeneracy of the $e_g(d_\pi)$ orbitals is calculated to be removed by the presence of the chelating water molecule by some 400 cm^{-1}, with the $e_g(d_\pi)$ ligand field orbital directed at the water protons lying lower. These results are demonstrated in Fig. 2, panels V and VI.

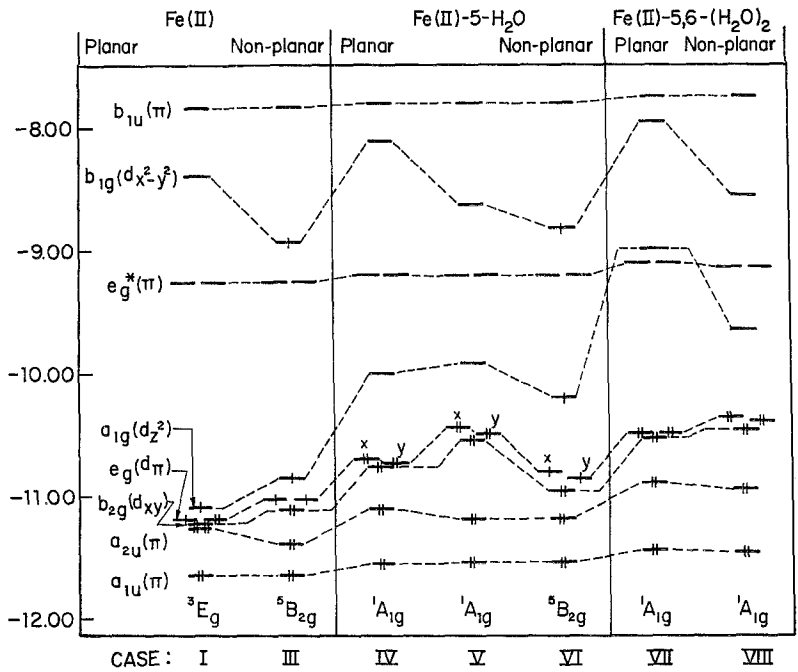

Fig. 2. Calculated Energies of Top Filled and Lowest Empty Orbitals: Ferrous Porphin and Ferrous Porphin Hydrates

The order of these three nearly degenerate ligand field orbitals d_{xy} and d_π is determined by the relative amounts of antibonding mixing ("antimixing") with the MO's of neighbors. The Fe $3d_{xy}$ orbital mixes only slightly, if at all, with the nitrogen $2p$ orbitals and insignificantly with the methine bridges. The two $3d_\pi$'s interact considerably more with not only the porphin π system, but also, because of non-planarity, with the porphin σ system. The $3d_\pi$ orbital which can antimix with the $2p\pi$ MO of water is further raised. Since most of the interactions are antibonding for these three orbitals in the cases under consideration, orbital energies are raised as metal purity decreases.

It is useful to compare these results with the investigations of GRIFFITH [*29*] on ferrihaemoglobin azide. From an examination of the EPR data of GIBSON and INGRAM [*23*], GRIFFITH deduces the same ligand field picture that we have derived here. GRIFFITH and KOTANI [*43, 44*] estimate the $3d_{yz} - 3d_{xz}$ orbital splitting to be 600 – 1500 cm^{-1} and the $3d_{xy} - 3d_{yz}$ splitting to be 600 – 1000 cm^{-1} for this azide, in good agreement with our results if we make the reasonable

Table 5. *Population Analysis of Top Filled and Lowest Empty* MO's

A: Porphin[a]

Case	$a_{2u}(\pi)$[b]				$e_{gx}(\pi)$[c]		$e_{gy}(\pi)$[c]	
	$3d_{z^2}$	$4p_\pi$	Ligand	Porphin π	$3d_{xz}$	Porphin π	$3d_{yz}$	Porphin π
I	—	0.03	—	0.97	0.02	0.98	0.02	0.98
II	0.18	0.02	—	0.79	0.01	0.99	0.01	0.99
III	0.24	0.02	—	0.72	0.01	0.99	0.01	0.99
IV	0.03	0.02	0.00	0.94	0.03	0.97	0.03	0.97
V	0.09	0.02	0.00	0.88	0.02	0.98	0.02	0.98
VI	0.16	0.03	0.01	0.79	0.01	0.99	0.01	0.99
VII	—	0.00	0.02	0.98	0.03	0.97	0.03	0.97
VIII	0.02	0.00	0.09	0.87	0.02	0.98	0.02	0.98
IX	0.07	0.03	0.02	0.87	0.01	0.99	0.01	0.99
X	0.15	0.04	0.04	0.75	0.01	0.99	0.01	0.99
XI	0.16	0.04	0.02	0.76	0.01	0.99	0.01	0.99
XII	0.11	0.02	0.00	0.86	0.01	0.99	0.01	0.99
XIII	0.02	0.00	0.13	0.83	0.00	0.99	0.01	0.99
XV	0.14	0.02	0.00	0.83	0.02	0.98	0.02	0.98
XVI	0.12	0.02	0.00	0.85	0.02	0.98	0.02	0.98

B: Ligand Field

Case	$b_{1g}(d_{x^2-y^2})$			$a_{1g}(d_{z^2})$						
	$3d_{x^2-y^2}$	$N(\sigma)$[d]	All Other	$3d_{z^2}$	$4s$	$4p_z$	$N(\sigma)$[d]	$N(\pi)$[d]	Ligands	All Others
I	0.55	0.40	0.05	0.90	0.05	–	0.04	—	—	0.01
II	0.57	0.35	0.08	0.76	0.03	0.01	0.01	0.09	—	0.10
III	0.55	0.38	0.07	0.70	0.03	0.01	0.01	0.13	—	0.12
IV	0.58	0.37	0.05	0.74	0.03	0.03	0.05	0.03	0.10	0.02
V	0.60	0.34	0.06	0.75	0.01	0.02	0.02	0.07	0.08	0.05
VI	0.54	0.39	0.07	0.64	0.01	0.02	0.02	0.13	0.09	0.09
VII	0.59	0.37	0.04	0.69	0.01	—	0.09	—	0.20	0.01
VIII	0.60	0.34	0.06	0.74	0.00	0.01	0.04	0.04	0.14	0.03
IX	0.55	0.38	0.07	0.44	0.00	0.13	0.04	0.12	0.20	0.07
X	0.46	0.46	0.08	0.48	0.00	0.03	0.03	0.18	0.16	0.12
XI	0.46	0.46	0.08	0.55	0.00	0.04	0.03	0.17	0.10	0.11
XII	0.58	0.34	0.08	0.60	0.00	0.10	0.03	0.11	0.08	0.08
XIII				0.58	0.00	0.02	0.07	0.07	0.18	0.08
XV				0.75	0.01	0.02	0.02	0.11	0.02	0.07
XVI				0.75	0.00	0.03	0.02	0.10	0.03	0.07

assumption that these orbital splittings decrease slightly upon going from ferric azide to ferrous hydrate*.

Calculations with water in both the fifth and sixth coordinating positions are also presented in Fig. 2. With the assumed geometries of Tab. 4, the indication is low spin for both Fe(II) in the porphin plane (Case VII) and 0.492 Å above the plane (Case VIII), but in the latter case just barely. A second water molecule added below the porphin plane can increase or decrease the $e_g(d_\pi)$ splitting, depend-

* From the results of Mössbauer spectroscopy an energy gap from $b_{1g}(d_{xy})$ to $e_g(d_\pi)$ of ~420 cm^{-1} has been deduced [24]. Because of the many assumptions of the derivation this result is rather approximate.

Table 5. B: Ligand Field (Continued)

Case	$e_g(d_{xz})$			$e_g(d_{yz})$			$b_{2g}(d_{xy})$	
	$3d_{xz}$	Ligands	Porphin	$3d_{yz}$	Ligands	Porphin	$3d_{xy}$	Porphi
I	0.86	—	0.14	0.86	—	0.14	0.97	0.03
II	0.90	—	0.10	0.90	—	0.10	0.98	0.02
III	0.88	—	0.12	0.88	—	0.12	0.98	0.02
IV	0.89	0.02	0.09	0.90	0.00	0.10	0.98	0.02
V	0.89	0.03	0.08	0.92	0.00	0.08	0.98	0.02
VI	0.83	0.05	0.12	0.87	0.00	0.13	0.98	0.02
VII	0.90	0.02	0.08	0.90	0.02	0.08	0.98	0.02
VIII	0.92	0.00	0.08	0.89	0.03	0.08	0.98	0.02
IX	0.82	0.07	0.11	0.82	0.07	0.11	0.98	0.02
X	0.65	0.14	0.21	0.65	0.14	0.21	0.96	0.04
XI	0.54	0.33	0.12	0.54	0.33	0.12	0.96	0.04
XII	0.76	0.14	0.10	0.76	0.14	0.10	0.98	0.02
XIII	0.36	0.53	0.10	0.72	0.11	0.16	0.79	0.05
XV	0.83	0.08	0.09	0.89	0.00	0.11	0.97	0.03
XVI	0.86	0.05	0.09	0.86	0.05	0.09	0.98	0.02

[a] The highest filled porphin $a_{1u}(\pi)$ MO is 100% porphin π in all cases.
[b] The population of the $4s$ in the porphin $a_{2u}(\pi)$ MO is less than 0.01 for all cases.
[c] The porphin $e_g^*(\pi)$ MO's have essentially no extension onto fifth and sixth position ligands.
[d] Total electronic population for all four porphin nitrogen atoms.

ing on whether it is added with the two water molecules in the same plane (C_{2v}) or perpendicular planes ($\sim S_4$). Examples of the latter are given by Cases VII and VIII.

As might be expected, the position of $a_{1g}(d_{z^2})$ relative to $e_g(d_\pi)$ is largely dependent on the fifth and sixth water molecules; also it is slightly dependent on iron geometry and spin state. The energy position of the $b_{1g}(d_{x^2-y^2})$ ligand field orbital relative to that of the $e_g(d_\pi)$ is mostly dependent on the location of the iron atom relative to the porphin plane, and is somewhat dependent on the electronic configuration. In the planar $S = 0$ complexes this energy gap averages $\sim$2.6 eV; with iron 0.492 Å out of plane, $S = 0$, $\sim$1.8 eV. This gap is consistently increased by $\sim$0.1 eV for $S = 1$ or 2 complexes.

The results of a population analysis on the principle ligand field orbitals is given in Tab. 5. The variation in metal purity among the hydrates is surprisingly small: $b_{2g}(d_{xy})$ is 97—98% pure; $e_g(d_\pi)$ is 83—92% pure; with the exception of the rather artificial planar ferrous with no ligands (Case I) which is 90% pure, $a_{1g}(d_{z^2})$ varies from 64—76%; finally $b_{1g}(d_{x^2-y^2})$ varies from 54—60% pure. Although $b_{2g}(d_{xy})$ remains pure except in the coplanar O_2 complex (Case XIII), the purity of the other d orbitals is generally lowered in ferric complexes (Cases IX, X, XI) and in ferrous complexes with CO (Case XII) and with coplanar O_2 (Case XIII).

A detailed investigation of electron distribution around the iron atom is given in Tab. 6. The total electronic populations for each atom of these ferrous porphin complexes is given in Tab. 7; the total π electron density in Tab. 8. We note that iron with $S = 2$ or $S = 1$ has a higher net charge by about 0.05 than the $S = 0$ case. Each water molecule 2.1 Å from the iron atom is calculated to have a net

Table 6. *Electronic Distribution of* Fe AO's

Case	I	II	III	IV	V	VI	VII	VIII	IX	X	XI	XII	XIII	XV	XVI
S	1	1	2	0	0	2	0	0	1/2	5/2	5/2	0	0	0	0
$3d_{x^2-y^2}$	0.896	0.824	1.439	0.829	0.768	1.436	0.808	0.772	0.881	1.518	1.518	0.802	1.004	0.875	0.839
$3d_{xy}$	1.994	1.996	1.996	1.994	1.996	1.996	1.994	1.996	1.995	1.034	1.033	1.996	1.996	1.974	1.995
$3d_{yz}$	1.527	1.515	1.110	1.940	1.954	1.100	1.931	1.952	1.496	1.332	1.439	1.700	1.982	1.961	1.858
$3d_{xz}$	1.527	1.515	1.110	1.940	1.953	1.139	1.931	1.953	1.496	1.332	1.439	1.700	1.240	1.834	1.858
$3d_{z^2}$	1.071	1.216	1.379	0.478	0.471	1.331	0.601	0.504	1.039	1.478	1.384	0.725	0.729	0.467	0.450
Total $3d$	7.015	7.066	7.034	7.181	7.142	7.002	7.265	7.177	6.907	6.694	6.814	6.922	6.951	7.111	7.000
$4s$	0.349	0.339	0.354	0.283	0.304	0.331	0.260	0.293	0.375	0.408	0.356	0.367	0.284	0.284	0.334
$4p_x$	0.139	0.136	0.140	0.125	0.133	0.144	0.114	0.126	0.144	0.164	0.166	0.141	0.174	0.141	0.135
$4p_y$	0.139	0.136	0.140	0.118	0.127	0.137	0.114	0.130	0.144	0.164	0.166	0.141	0.168	0.130	0.135
$4p_z$	0.135	0.103	0.106	0.114	0.134	0.173	0.096	0.124	0.221	0.304	0.249	0.261	0.124	0.126	0.213
Total $4p$	0.413	0.375	0.386	0.357	0.394	0.454	0.323	0.380	0.509	0.532	0.581	0.543	0.466	0.396	0.483
Total	7.778	7.780	7.774	7.821	7.839	7.787	7.849	7.850	7.792	7.735	7.751	7.832	7.700	7.791	7.818
Net	0.222	0.220	0.226	0.179	0.161	0.213	0.151	0.150	0.208	0.265	0.249	0.168	0.300	0.209	0.182

Table 7. *Total Electronic Population*

	I	II	III	IV	V	VI	VII	VIII
H (1)	0.941	0.941	0.942	0.945	0.945	0.944	0.948	0.948
C (2)	4.046	4.047	4.048	4.060	4.056	4.057	4.064	4.058
C (3)	3.979	3.977	3.977	3.985	3.984	3.984	3.989	3.986
H (4)	0.922	0.918	0.918	0.926	0.923	0.923	0.932	0.928
C (5)	4.031	4.026	4.022	4.038	4.032	4.033	4.037	4.035
C (6)	3.979	3.977	3.977	3.985	3.984	3.984	3.989	3.987
C (7)	4.046	4.047	4.048	4.060	4.056	4.057	4.064	4.058
H (8)	0.941	0.941	0.942	0.945	0.945	0.944	0.948	0.948
N (9)	5.170	5.179	5.183	5.176	5.185	5.197	5.195	5.195
N (10)	5.170	5.179	5.183	5.176	5.185	5.197	5.195	5.195
Total	112.220	112.220	112.224	112.480	112.440	112.492	112.656	112.566
Net Porphin	−0.220	−0.220	−0.224	−0.480	−0.440	−0.492	−0.656	−0.566
Net Fe	0.222	0.220	0.226	0.179	0.161	0.213	0.151	0.150
Ligand	–	–	–	H_2O	H_2O	H_2O	H_2O (5)	H_2O (5)
				H/0.697	H/0.708	H/0.702	H/0.708	H/0.710
				O/6.309	O/6.303	O/6.322	O/6.332	O/6.306
							H_2O (6)	H_2O (6)
							H/0.708	H/0.729
							O/6.332	O/6.399
Net Ligand	–	–	–	0.298	0.281	0.274	0.504	0.417

Table 7. (Continued)

	IX	X	XI	XII	XIII	XV	XVI
H (1)	0.940	0.941	0.942	0.942	0.940	0.941	0.941
C (2)	4.047	4.039	4.048	4.051	4.046	4.050	4.050
C (3)	3.970	3.970	3.976	3.976	3.968	3.971	3.975
H (4)	0.923	0.914	0.918	0.921	0.918	0.913	0.914
C (5)	4.005	4.022	4.016	4.021	4.020	4.041	4.036
C (6)	3.970	3.970	3.976	3.976	3.961	3.970	3.975
C (7)	4.047	4.039	4.048	4.051	4.041	4.050	4.050
H (8)	0.940	0.941	0.942	0.942	0.940	0.941	0.941
N (9)	5.149	5.182	5.193	5.160	5.142	5.159	5.178
N (10)	5.149	5.182	5.193	5.160	5.163	5.172	5.178
Total	111.961	111.826	112.241	112.168	111.951	112.161	112.240
Net Porphin	+0.039	−0.075	−0.241	−0.168	+0.049	−0.161	−0.241
Net Fe	0.208	0.265	0.249	0.168	0.300	0.209	0.182
Ligand	CN	Cl	OH	CO	O_2 (5)	N_2	N_2
	C/4.041	7.190	H/0.709	C/3.910	O/6.267	N/5.024	N(N-Fe)
	N/5.205		O/6.299	O/6.091			4.943
					H_2O (6)		N/4.997
					H/0.716		
					O/6.382		
Net Ligand	−0.246	−0.190	−0.008	−0.001	−0.348	−0.048	+0.060

Table 8. *π Electronic Populations*

	I	II	III	IV	V	VI	VII
S	1	1	2	0	0	2	0
C(2)	1.004	1.007	1.004	1.019	1.015	1.011	1.024
C(3)	1.054	1.053	1.054	1.060	1.058	1.057	1.063
C(5)	0.961	0.949	0.938	0.967	0.957	0.957	0.973
C(6)	1.054	1.053	1.054	1.060	1.058	1.058	1.063
C(7)	1.004	1.007	1.004	1.019	1.015	1.012	1.024
N(9)	1.375	1.351	1.307	1.368	1.340	1.323	1.380
N(10)	1.375	1.351	1.307	1.368	1.340	1.322	1.380
Fe[a]	3.190	3.133	2.326	3.994	4.041	2.412	3.958
Total Porphin	25.808	25.680	25.444	25.972	25.772	25.670	26.108

	VIII	IX	X	XI	XII	XIII	XV	XVI
S	0	1/2	5/2	5/2	0	0	0	0
C(2)	1.018	1.005	1.005	1.012	1.011	1.007	1.013	1.013
C(3)	1.061	1.050	1.063	1.066	1.054	1.050	1.061	1.063
C(5)	0.966	0.938	0.955	0.954	0.947	0.948	0.962	0.962
C(6)	1.061	1.050	1.063	1.066	1.054	1.049	1.061	1.063
C(7)	1.018	1.005	1.005	1.012	1.011	1.006	1.013	1.013
N(9)	1.351	1.345	1.310	1.309	1.340	1.388	1.307	1.312
N(10)	1.350	1.345	1.310	1.309	1.340	1.370	1.306	1.312
Fe[a]	4.029	3.213	2.968	3.127	3.660	3.345	3.921	3.930
Total Porphin	25.898	25.572	25.605	25.676	25.668	25.756	25.666	25.704

[a] Total of $4p_z$ and two $3d_\pi$ AO's; for detailed structure, see Tab. 6.

positive charge of 0.25 – 0.30 electrons. The water molecule 2.6 Å from the iron atom is much more neutral, +0.14. It is difficult from these investigations to pinpoint any one atomic location in the porphin moiety responsible for changes in the net electronic populations of the porphin ring.

b) Ferric Porphin Complexes (Cases IX, X, XI)

We report here the results of calculations on three ferric porphin complexes; that of CN^-, Cl^- and OH^-. Ferric porphin cyanide (Case IX) is calculated to have a ^2E_g ground state

$$(b_{2g})^2 (e_g)^3 .$$

Low spin in this complex can be mostly attributed to the greatly raised orbital energy of the $a_{1g}(d_{z^2})$ MO, strongly antibonded with the CN^- sigma orbitals. This $a_{1g}(d_{z^2})$ MO is only 44% metal $3d_{z^2}$ and is estimated to be 20% on CN^-, over twice as much density on the fifth position ligand as that found in the hydrated ferrous cases.

Both the ferric chloride (Case X) and ferric hydroxide (Case XI) complexes are calculated to have high spin $^6A_{1g}$ ground states

$$(b_{2g})^1 (e_g)^2 (a_{1g})^1 (b_{1g})^1 .$$

This electronic assignment, however, is not without ambiguity as the strong covalency calculated for the ligand field orbitals probably makes our estimates of exchange integrals too large. This is especially marked in the hydroxide complex (Tab. 5). Surpressing for the moment this complication to our model, the ligand field strengths of these two counter-ions, as measured by the gained stability of the high spin electronic configuration over that of the low spin, are predicted nearly the same.

Quite apparent from Fig. 3 is the larger $e_g(d_\pi) - b_{2g}(d_{xy})$ orbital energy gap calculated for these high spin complexes. For the hydroxide complex this

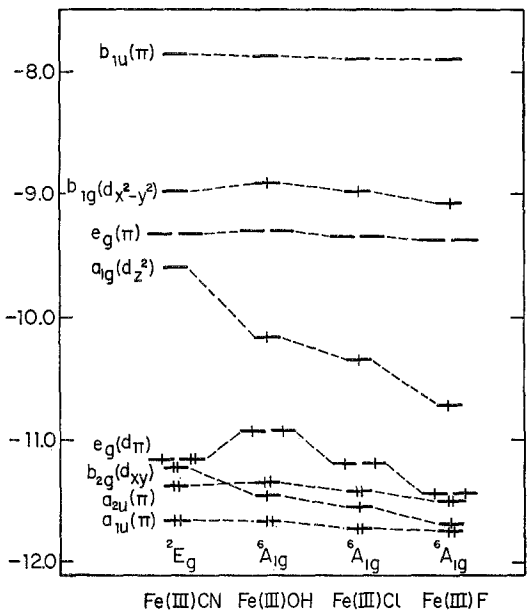

Fig. 3. Calculated Energies of the Top Filled and Lowest Empty Orbitals of Ferric Porphin Complexes

is caused by a large antibonding interaction with lower lying OH^- $2p_\pi$ orbitals, causing "repulsion". The effect is less noted for the chloride complex in which the Cl^- $2p_\pi$ orbitals are lower lying than those of OH^-. We have included in Fig. 3 the results of a fluoride calculation in which the $e_g(d_\pi) - b_{2g}(d_{xy})$ orbital energy difference is small. In this case the $2p_\pi$ orbitals of fluoride are much lower in energy, and are essentially filled basis orbitals. We do not detail the fluoride calculation here as the large negative charge on fluorine of -0.44 places some doubt on the use of a neutral atom basis set.

Tab. 5 demonstrates the amount of metal $3d$ character in these "ligand field" orbitals. In general, the metal orbitals in ferric complexes appear to be mixed to a greater extent than those of ferrous, especially in the high spin complexes. These orbitals have mixed not only with the porphin orbitals, but also to a great extent with those of the negative counter-ion.

The calculated orbital energy differences between the $e_g(d_\pi)$ and $b_{1g}(d_{x^2-y^2})$ orbitals lie between 2.0 and 2.2 eV, somewhat greater than that encountered in

the non-planar ferrous cases. This is expected as we have placed the iron atom more into the porphin plane for the ferric calculations [37].

Tab. 6 shows the detailed electronic structure of the iron orbitals. Again the net charge in the high spin complexes, 0.25—0.26, is greater than that found for the low spin, 0.21, by about 0.05, which is the same order of magnitude as the difference between ferrous and ferric both being low (or high) spin. Electrons, formally lost from the $3d$ shell in ferric, have been gained back indirectly through greater $3d$ mixing with the filled orbitals of the negative counterions.

The net charges calculated on the negative ions are -0.44 for F, -0.25 for CN, -0.19 for Cl and -0.01 for OH.

c) Further Complexes of Ferrous Porphin

1. Carbon Monoxide (Case XII)

The addition of carbon monoxide vertically above the iron atom in ferrous porphin is calculated to cause a low spin ligand field, as is observed [57, 33]. The

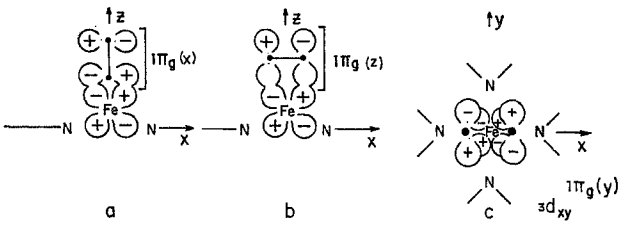

Fig. 4. Important Fe-Ligand Interactions

$3d_{z^2}$ orbital of Fe "antimixes" with the sigma orbitals of CO, increasing the orbital energy gap between the $a_{1g}(d_{z^2})$ and $e_g(d_\pi)$ to almost 1.5 eV. This might be compared with the 0.6 eV orbital gap introduced upon addition of a single water molecule to the free compound, calculated by this model to *just* maintain high spin. Correspondingly, the metal $3d_{z^2}$ purity of this $a_{1g}(d_{z^2})$ MO has decreased from 70% to 60%.

Of interest is the apparent reversal in this calculation of the energy order of the $e_g(d_\pi)$ and $b_{2g}(d_{xy})$ ligand field orbitals, brought about by the relatively strong bonding of the Fe $3d_\pi$'s with the unoccupied $1\pi_g$ MO's of CO, Fig. 4a*. The $e_g(d_\pi)$ ligand field orbitals are calculated 0.2 eV below the $b_{2g}(d_{xy})$. The metal character of the $e_g(d_\pi)$ orbitals has decreased from 88% in the free compound to 76%; the electronic shift represented is to CO.

The behavior of the $b_{2g}(d_{xy})$ and the $b_{1g}(d_{x^2-y^2})$ MO's is not much changed by the addition of CO, as expected, for the ligand contains no orbitals of the proper symmetry to mix.

The net charge found on the iron atom is in agreement with the previous low spin ferrous calculations. The carbon monoxide molecule is calculated to be almost neutral in this complex.

The orbital energy pattern obtained is given in Fig. 5 along with the free compound for comparison. Quite striking is the appearance for the first time of MO's

* We have used the label $1\pi_g$ appropriate to $D_{\infty h}$, even though CO has lower symmetry, to note its correspondence to similar orbitals in O_2 and N_2.

lying in orbital energy between that of the porphin $e_g^*(\pi)$ and porphin $b_{1u}(\pi)$. These new MO's consist mostly of the CO $1\pi_g$ orbital antibonded to the Fe $3d_\pi$'s, and might be considered as the antibonding partners of the principal $e_g(d_\pi)$ ligand field orbitals.

2. Oxygen (Cases XIII and XIV)

In an attempt to simulate the biologically active oxygenated ferrohaemoglobin, oxygen was added 2.1 Å from the iron atom of hydrated ferrous porphin in two geometric configurations; one with the oxygen axis parallel to the X axis of

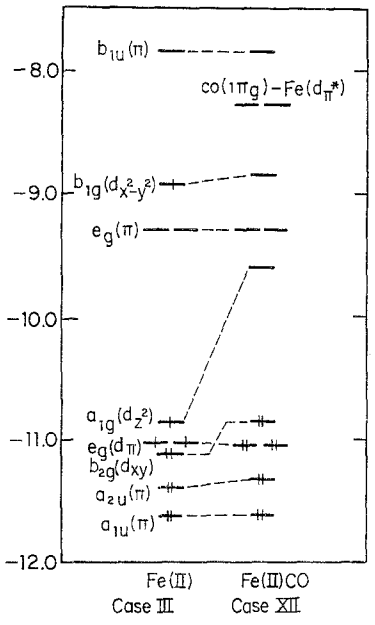

Fig. 5. CO Ferrous Porphin

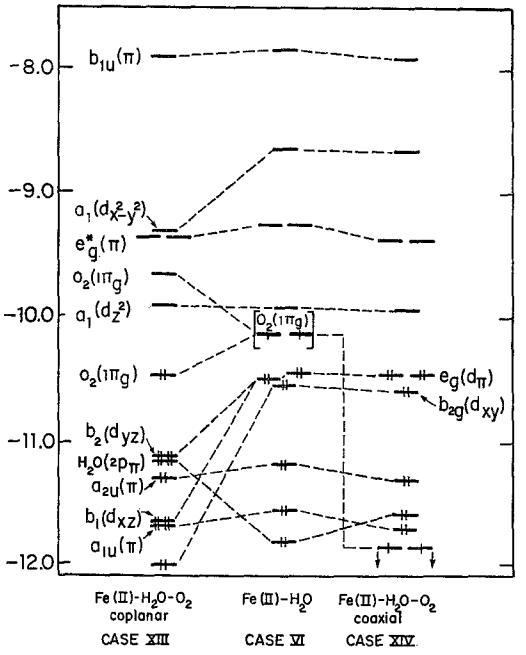

Fig. 6. Oxyferroporphins

the porphin plane, centered over the iron atom and passing over two "opposite" porphin nitrogens (coplanar), and the other centered above the iron atom and perpendicular to the porphin plane (coaxial). Since our computer programs required the complex to have at least C_{2v} symmetry, less symmetrical orientations could not be investigated.

Coplanar oxyferroporphin monohydrate is predicted to be diamagnetic, in accord with experiment [57]. The metal character of the $a_1(d_{x^2-y^2})$, $a_1(d_{z^2})$ and $b_2(d_{yx})$ are much the same as in the carbonyl complex. The calculated orbital gap between the $b_2(d_{xy})$ and $a_1(d_{z^2})$ is 1.2 eV. The metal $3d_{xz}$ orbital has so mixed with the 0_2 $1\pi_g(Z)$ MO, directed into the porphin plane, that no MO of the complex can be accurately described as a $3d_{xz}$ metal orbital in a ligand field (Fig. 4b). The $a_2(d_{xy})$ MO has been lowered by considerable bonding with the O_2 $1\pi_g(Y)$ MO, directed parallel to the porphin plane, Fig. 4c. This orbital is but 80% Fe $3d_{xy}$ in strong contrast to its 97—98% pure metal character calculated for all the other complexes considered in this paper. The two $1\pi_g$ MO's of diatomic oxygen, each

singly occupied in the paramagnetic free molecule, are calculated split by some 6600 cm^{-1}, the $1\pi_g(Z)$ lying highest. These results are presented in Fig. 6.

The net Fe charge in this environment is calculated to be +0.30, considerably higher than in any of the other complexes we have considered, and, indeed, even those formally ferric. The oxygen molecule is estimated to have a net charge of −0.53. The water molecule, 2.6 Å below Fe, has a net charge of +0.18, not too different from the +0.14 value found for the similarly situated water of ferrous dihydrate (Case VIII).

That the coaxial structure should be paramagnetic and hence cannot correspond to oxyferrohaemoglobin, which is diamagnetic, was pointed out by GRIFFITH [28]. Our own calculations show the same result in Fig. 6, where it is seen that the $1\pi_g$ orbitals remain degenerate and singly occupied. However, the present calculations give a second result, for the $1\pi_g$ orbitals are so far below the occupied orbitals $e_g(d_\pi)$ and $b_{2g}(d_{xy})$, that we would expect an electron transfer $e_g(d_\pi) \rightarrow 1\pi_g$. Indeed, it is known that unprotected ferrous porphyrin is subject to immediate oxidation by air [72]. The present calculations suggest, therefore, that the coaxial geometry is chemically unstable*.

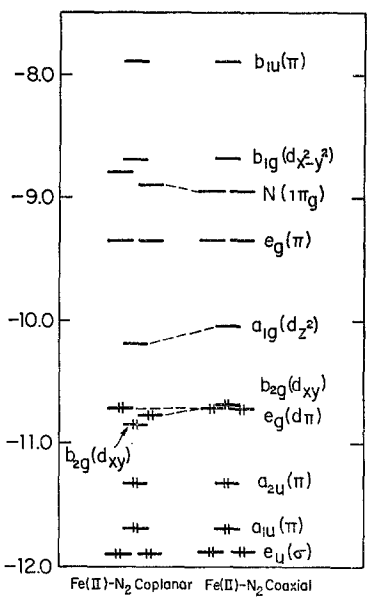

Fig. 7
The Effect of Diatomic Nitrogen on Ferrous Porphin

3. *Nitrogen (Cases XV and XVI)*

The addition of diatomic nitrogen to a coplanar position 2.1 Å above the central Fe(II) atom is predicted to produce a low spin ground state. The occupied MO's of nitrogen lie well below the top filled porphin orbitals. The unoccupied $1\pi_g$ nitrogen MO's lie above the porphin $e_g^*(\pi)$'s, and, unlike in the coplanar oxygen complex, are nearly degenerate, Fig. 7. The two principal $e_g(d_\pi)$ ligand field orbitals are split in orbital energy by 500 cm^{-1}, slightly greater than the splitting calculated for the monohydrate. Again, the $3d_\pi$ orbital which can antimix with the filled $1\pi_u$ orbital of the ligand lies highest. The $b_{2g}(d_{xy})$ lies 600 cm^{-1} below the lowest $e_g(d_\pi)$. The $b_{2g}(d_{x^2-y^2})$ orbital is calculated to lie 1.97 and 2.03 eV above the two $e_g(d_\pi)$'s; the $a_{1g}(d_{z^2})$, 0.53 and 0.59 eV above the two $e_g(d_\pi)$'s. The net ligand field produced is only slightly stronger than that estimated for non-planar ferrous monohydrates.

N_2 complexing in a coaxial geometry does not appear to greatly alter the results obtained for the coplanar case, as demonstrated in Fig. 7. Orbital degeneracy is, of course, maintained. The ligand field strength is estimated to be somewhat

* The electron assignment of Fig. 6 was also unstable for our computer programs; the orbitals $1\pi_g$ were so low, that the program insisted on filling them. The energies in Fig. 6 are therefore extrapolated.

stronger, as the $a_{1g}(d_{z^2}) - e_g(d_\pi)$ energy gap has increased to 0.66 eV; the b_{1g} $(d_{x^2-y^2}) - e_g(d_\pi)$ gap is 2.04 eV. Most notable is the reversal in orbital energy of the $e_g(d_\pi)$ and $b_{2g}(d_{xy})$, similar to that calculated for the isoelectronic CO complex. However, in this case the orbital energy difference is but 180 cm^{-1} compared to the 1600 cm^{-1} value calculated for the CO complex.

The nitrogen molecule in both coplanar and coaxial complexes is calculated to be nearly neutral; in the former case, −0.05, and in the latter, +0.06. The net charge on the iron atom is calculated to be +0.21 and +0.18, respectively. These values are somewhat intermediate when compared with the results of the high and low spin ferrous porphin hydrates.

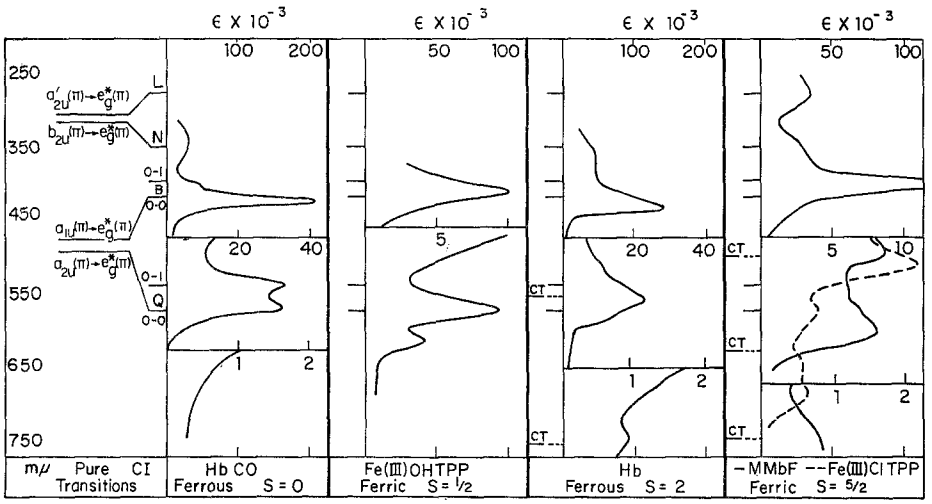

Fig. 8. Some Spectra of Iron Porphin Comples: Hb = Haemoglobin, MMb = Met- or Ferri-myoglobin, TPP = Tetraphenylporphyrin; HbCO and Hb spectra, [*21*]; Fe(III) OHTPP and Fe(III)Cl TPP [*16*]; MMbF visible and red [*22*]; ultraviolet [*31*]

The MO's of diatomic nitrogen in both these cases have mixed only slightly with the orbitals of porphin and of Fe. There is a net negative overlap population between the iron porphin and the N_2 suggesting that no stable complex forms [*52*].

d) Electronic Transitions

1. Empirical characterization

Fig. 8 gives the visible and the near ultraviolet spectra of some iron porphyrins that illustrate the basic spectral types. Fig. 9 gives some ferrous hemoglobin spectra on a logarithmic scale and also shows the near infrared region. More detailed spectra are given elsewhere [*22, 16, 39, 40*]. The spectral types are classified according to iron oxidation state and spin and have the following characteristics:

(i) Ferrous $S = 0$: The CO complex of ferrous iron is low spin. As shown in Fig. 8 and 9 it has two bands in the visible and very strong sharp Soret band in the near ultraviolet. Although Fig. 9 shows some very weak absorption in the 700—1000 mμ, range, this may well be some type of impurity. The visible peaks, called the α and β bands, are known to sharpen at low temperature [*19*]. Drabkin [*16*]

has pointed out that the two banded visible spectra differ among the following ferrous low spin cases: the CN^- complex has α more intense than β, for the CO complex α and β have roughly equal intensity, while for the pyridine complex α is less intense than β. The β bands are all about the same intensity.

The O_2 complex, though $S = 0$, shows one unusual feature in Fig. 9, a band at $\lambda \approx 900$ mμ. In this respect it is unique among ferrous low spin spectra.

(ii) Ferric ($S = \frac{1}{2}$): The OH^- complex of ferric tetraphenylporphin is given as a particularly clear illustration of ferric low spin, although in the haemoproteins the hydroxide complex, may be mixed high and low spin [*22*]. The two banded visible spectrum is particularly sharp in Fig. 8, although the same two bands

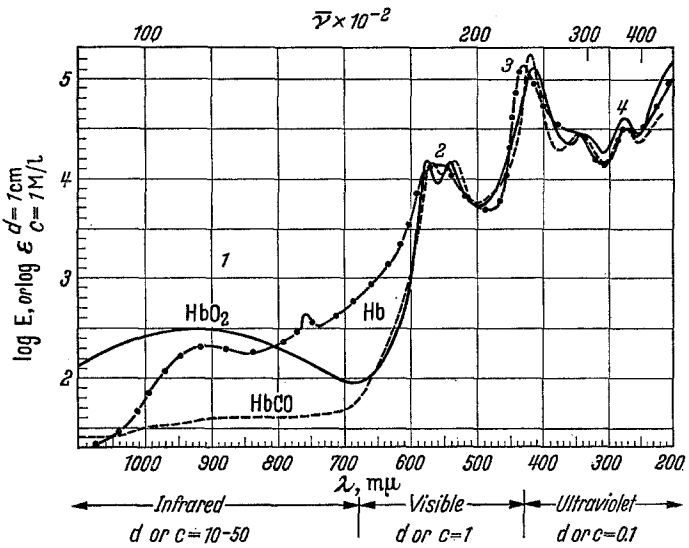

Fig. 9. Absorption spectra of oxyhaemoglobin, HbO_2, deoxygenated haemoglobin, Hb, and carbonyl haemoglobin, HbCO. The d and c values refer to curvette thickness, d, or concentration, c, for optimal spectrophotometry [*16*]

broadened are observable in other spectra*. The ferric CN^- complex appears to have no near infrared absorption [*22*].

(iii) Ferrous ($S = 2$): As shown in Fig. 8, high spin ferrous gives a similar visible-ultraviolet spectrum to the two low spin cases, but the bands are even more broadened. There are probably three bands in the visible. The Soret band is skewed. These compounds have some absorption in the near infrared (900 mμ) as shown by free hemoglobin in Fig. 9.

(iv) Ferric ($S = \frac{5}{2}$): There appear to be two spectral types* for ferric high

* The reader is referred to KEILIN and HARTREE ([*39*], Figs. 1 and 2 and [*40*], Fig. 9) for clear illustrations of visible-ultraviolet spectra. The reduced peroxidase CO and CN^- spectra are ferrous ($S = 0$). The reduced peroxidase (free) is ferrous ($S = 2$). The peroxidase CN^- complex is ferric ($S = \frac{1}{2}$) and the free peroxidase and the peroxidase F^- complex give the two types of ferric ($S = \frac{5}{2}$) spectra. See also Ref. [*22*] Figs. 4 to 8 for ferric high and low spin spectra in the near infrared, visible, and near ultraviolet. The spin state of FeOHTPP, shown in Fig. 8 as low spin, has not been determined, although the spectrum is that of low spin. Our calculations show that if the iron is out-of-plane high spin is expected. It may be that in benzene solution the iron in FeOHTPP moves towards the plane, thus changing the spin state.

spin shown in Fig. 8. Both types show evidence for several bands in the visible region, although the bands are broad. They also show bands in the near infrared [*22*].

2. $\pi \rightarrow \pi^*$ transitions

Much of the theoretical study and experimental study of porphyrins have been devoted to $\pi \rightarrow \pi^*$ transitions. Almost all metal porphyrins are characterized by the following "normal" spectrum: It has no absorption in the near infrared, it shows two bands with sometimes a weak third, in the visible, and the strong Soret band in the near ultraviolet [*25, 15*]. The first (low energy) visible band can vary in intensity. It seems clear that the ferrous ($S = 0$) spectra (with the exception of the O_2 complex) are of this "normal" type.

The theoretical origin of the "normal" visible-ultraviolet bands is ascribed to orbital transitions $a_{2u}(\pi) \rightarrow e_g^*(\pi)$ and $a_{1u} \rightarrow e_g^*(\pi)$ [*26, 74, 25*]. However these transitions are nearly degenerate in energy and are heavily mixed because of electron interaction. The resultant excited states are a low energy Q state, in which the transition dipoles of the basic orbital transitions nearly cancel, and a higher energy B state, in which the transition dipoles add. In this way the intensity difference between the visible and Soret bands can be explained [*26, 74, 25, 60*].

Although the higher oxidation states of Mn porphyrins show visible-ultraviolet spectra quite different from this "normal" pattern [*48, 8*] it is clear from Fig. 8 and 9 that in iron complexes the "normal" spectrum, though sometimes broadened and sometimes augmented by extra bands in the visible and near infrared, is preserved. The present calculations show how this works.

Focusing our attention first on the empty $e_g^*(\pi)$ MO's we note that no additional ligands split the degeneracy of these orbitals by more than 2 cm^{-1}, save coplanar bound N_2 and O_2 where the splitting is less than 80 cm^{-1}. Tab. 5A indicates that these MO's are almost entirely built up of π symmetry basis orbitals in spite of non-planarity, and are never more than 3% metal $3d_\pi$.

The highest filled $a_{1u}(\pi)$ orbital, with nodes through the methine bridges and through the four porphin nitrogens, cannot mix with any of the metal basis orbitals. Although this MO could conceivably combine with the orbitals of coplanar O_2 or N_2 it does not. It is 100% of π symmetry in all cases and is only affected by small differences in the self consistent charge fields established for these complexes. The average dipole for the $a_{1u}(\pi) \rightarrow e_g^*(\pi)$ transition is estimated to be 2.2 Å and only varies by ± 0.02 Å for all the cases considered.

The $a_{2u}(\pi)$ MO appears to be more sensitive to the central metal and its geometry, and to additional ligands. An examination of Tab. 5A shows that nonplanarity can mix considerable amounts of Fe $3d_{z^2}$ into the $a_{2u}(\pi)$. Some ligand character has also entered this porphin orbital and is especially marked in the coplanar oxyferroporphin monohydrate complex (Case XIII). The net result of the extension of this MO outside of the porphin moiety is to produce an orbital that is sensitive to the spin state of the central iron atom, averaging $96 \pm 2\%$ pure "porphin π" for planar situations, but decreasing to $86 \pm 3\%$ for nonplanar low spin complexes and $76 \pm 3\%$ for non-planar high spin complexes. In spite of these rather different compositions of the $a_{2u}(\pi)$ orbital the transition dipole to the $e_g^*(\pi)$ is calculated to vary only between 2.0 and 2.1 Å.

According to the method in which we have chosen the interaction parameter $\varkappa$, energy differences between these π orbitals correspond to the differences in energy between the average singlet-triplet excitation of the pure configurations. As mentioned previously in the discussion of method, the meaningful quantity to examine is the average transition energy of the two lowest lying excitations. For ferrous complexes this value is 2.15 ± 0.07 eV; for those of ferric, 2.22 ± 0.02 eV. These numbers should be compared with the 2.19 eV experimental average of Co, Ni, Cu and Zn tetraphenylporphyrins for which $\varkappa$ was fit.

The conclusion is that different transition metals in the central cavity, their relation to the porphin plane, and additional fifth and sixth position ligands above and below the central metal may have subtle influences not predictable by this molecular model, but do in no way affect the main characteristic features of the porphyrin $\pi \rightarrow \pi^*$ spectrum observed in the visible and near UV.

In a similar manner to that outlined for the Q and B bands, the N and L bands of porphyrins, appearing to the blue of the B, have been attributed by the SCMO–PPP calculations of Paper IV to heavily mixed transitions arising from nearly degenerate $b_{2u}(\pi)$ and $a'_{2u}(\pi)$ MO's lying below the top filled $a_{1u}(\pi)$. As the $a'_{2u}(\pi) \rightarrow e^*_g(\pi)$ transition is estimated to have a considerably larger dipole than that of the $b_{2u}(\pi) \rightarrow e^*_g(\pi)$, heavy mixing of these two pure excited configurations give two transitions of near equal probability, as is observed [9].

The SCC–EH calculations on iron porphin complexes again verify this general analysis. However, these calculations do demonstrate some sensitivity of the $a'_{2u}(\pi)$ and $b_{2u}(\pi)$ MO's, both with large electronic density on the four porphin nitrogens, to the location of the metal atom relative to the porphin plane. In the planar cases considered, these orbitals lie within 0.23 eV of one another. In the non-planar cases this energy gap is somewhat increased and considerable mixing has developed between the $b_{2u}(\pi)$ MO and a near $b_{1g}(\sigma)$, the latter lying in orbital energy between that of the $a'_{2u}(\pi)$ and $b_{2u}(\pi)$. These two orbitals, $b_{1g}(\sigma)$ and $b_{2u}(\pi)$, both of b_1 symmetry in C_{4v}, appear insensitive to addition of fifth and sixth position ligands.

The $a'_{2u} \rightarrow e^*_g(\pi)$ transition has an estimated dipole of ~0.4 Å for all these cases. The $b_{2u}(\pi) \rightarrow e^*_g(\pi)$ transition has a maximum dipole of ~0.1 Å for the planar cases, a value which is expected to decrease with increasing $b_{1g}(\sigma)$ mixing. Similarly, the $b_{1g}(\sigma) \rightarrow e^*_g(\pi)$ transition would become allowed as the $b_{1g}(\sigma)$ MO gains π character.

3. Charge Transfer Transitions

The present calculations suggest many electronic transitions which have charge transfer behavior in that such transitions would result in a shift of sizeable electronic density from one part of the porphin complex to another. Although sharp delineations cannot easily be made in a molecular orbital description of such transitions, they can, for our purposes, be considered to fall into three major categories: 1. between porphin and iron, 2. between iron and additional ligands, and 3. between porphin and ligands.

Most apparent of such transitions are those involving the vacant ligand field orbitals of the central iron atom. Foremost among these are excitations from the

top filled porphin π orbitals. The transitions allowed and hence perhaps observable in D_{4h} symmetry are:

$$\left.\begin{matrix} a_{2u}(\pi) \\ a_{1u}(\pi) \\ b_{2u}(\pi) \\ a'_{2u}(\pi) \end{matrix}\right\} \xrightarrow{x,y} e_g(d_\pi)$$

$$\left.\begin{matrix} a_{2u}(\pi) \\ a'_{2u}(\pi) \end{matrix}\right\} \xrightarrow{z} a_{1g}(d_{z^2})$$

$$b_{2u}(\pi) \xrightarrow{z} b_{1g}(d_{x^2-y^2}) .$$

In the absence of other influences, however, such transitions should be weak as the MO's involved are concentrated in different regions of the molecular complex.

In the low spin complexes of ferrous porphin, only the z polarized transitions to the ligand field $a_{1g}(d_{z^2})$ and $b_{1g}(d_{x^2-y^2})$ are possible. The ground state is $^1A_{1g}$. The excited states are $^3A_{2u}$'s and $^1A_{2u}$'s of which, of course, only the latter should have intensity. Employing the model developed for transition energies, these excitations are estimated by

$$\Delta E(^1A_{1g} \rightarrow {}^{3,1}A_{2u}) = w(i) - w(p) \mp K_{ip}$$

where i refers to the ligand field orbital and p refers to those of porphin. Ignoring the exchange between an electron and hole restricted mainly to different parts of the molecular complex, these transitions are estimated by a simple orbital energy difference. Transitions to the $a_{1g}(d_{z^2})$ ligand field orbital are, of course, sentitive to the nature of additional ligands. If the ferrous complex is of low spin, then the energy of the $a_{2u}(\pi) \rightarrow a_{1g}(d_{z^2})$ transition is estimated to be at least 1.2 eV, or in the IR. In the carbonyl complex this transition is estimated to be as high as 1.7 eV, in the near red to visible region. Corresponding transitions from the $a'_{2u}(\pi)$ MO are estimated to be ~1.2 eV higher in energy. The energy of the $b_{2u}(\pi) \rightarrow b_{1g}(d_{x^2-y^2})$ transition is sensitive to the position of the iron atom relative to the porphin plane and is estimated by these calculations to lie at ~4.0 eV in the planar cases and 3.2 eV in the non-planar.

In the low spin ferric compounds there is one electron hole in the three nearly degenerate ligand field $e_g(d_\pi)$ and $b_{2g}(d_{xy})$ ligand field orbitals, giving rise to possible ground states of ^2E_g or $^2B_{2g}$ symmetry. The ^2E_g state is predicted to lie slightly lower in our ferric cyanide calculation, but the apparent reversal of the order of the $e_g(d_\pi)$ and $b_{2g}(d_{xy})$ orbitals in the low spin ferrous carbonyl and coaxial N_2 calculations is suggestive. If the hole does, indeed, lie in the $e_g(d_\pi)$ orbital, then transitions to this orbital are possible. Such $^2E_g \rightarrow {}^2X_u$ ($X = A_1$, A_2, B_1 or B_2) transitions are estimated by orbital energy differences

$$\Delta E(^2E_g \rightarrow {}^2X_u) = w(e_g) - w(p) .$$

These estimates are presented in Tab. 9. Transitions from the $a_{2u}(\pi)$ and $a_{1u}(\pi)$ and from the $b_{2u}(\pi)$ and $a'_{2u}(\pi)$, always lying in near degenerate pairs, might again be expected to mix through CI as they did in forming the visible and UV spectrum. As these transitions are of (x,y) polarization the higher energy pair might borrow intensity from the visible and Soret bands.

Excitations to an $a_{1g}(d_{z^2})$ or $b_{1g}(d_{x^2-y^2})$ orbital from the porphin π system in low spin ferric complexes leads to a quartet and two doublets, the quartet excitation being spin forbidden. The excitation energy of the two doublets is given by

$$\begin{aligned}\Delta E(^2E_g \to {}^2E_u) &= w(i) - w(p) + \tfrac{1}{3}(K_{pb} + K_{pi} + K_{bi}) + \\ &\quad + (K_{pb}^2 + K_{pi}^2 + K_{bi}^2 - K_{pb}K_{pi} - K_{pb}K_{bi} - K_{pi}K_{bi})^{1/2} \\ \Delta E(^2E_g \to {}^2E_u) &= w(i) - w(p) + \tfrac{1}{3}(K_{pb} + K_{pi} + K_{bi}) - \\ &\quad - (K_{pb}^2 + K_{pi}^2 + K_{bi}^2 - K_{pb}K_{pi} - K_{pb}K_{bi} - K_{pi}K_{bi})^{1/2}\,.\end{aligned}$$

Again, considering exchange integrals between metal and porphin MO's small, especially when compared with those between two metal orbitals, these transitions are estimated by

$$\begin{aligned}\Delta E(^2E_g \to {}^2E_u) &\approx w(a_{1g}) - w(a_{2u}) + 0.62\ (-0.31) \\ \Delta E(^2E_g \to {}^2E_u) &\approx w(b_{1g}) - w(b_{2u}) + 0.88\ (-0.44)\end{aligned}$$

where the values in parenthesis refer to the primed states above. The $a_{2u}(\pi)$ and $a'_{2u}(\pi) \to a_{1g}(d_{z^2})$ transitions are thus estimated to lie at 2.4 and 1.5 eV and 3.5 and 2.6 eV respectively, in the visible and Soret region; the $b_{2u}(\pi) \to b_{1g}(d_{x^2-y^2})$ excited doublets are estimated at 4.1 and 2.8 eV, buried in the UV. The former transitions will be sensitive to fifth and sixth position ligands and the latter to the relation of the iron atom to the porphin plane.

High spin ferrous complexes are predicted to have a $^5B_{2g}$ ground state, although, again, the three nearly degenerate ligand field orbitals suggest the possibility of a low lying ^5E_g. Assuming the $^5B_{2g}$ state as lowest, transitions from the $a_{2u}(\pi)$ and $a_{1u}(\pi)$, and $b_{2u}(\pi)$ and $a'_{2u}(\pi)$ to the $e_g(d_\pi)$ are estimated by

$$\Delta E(^5B_{2g} \to {}^5E_u) = w(e_g) - w(p) + \tfrac{2}{3}(K_{bc} + K_{bd} + K_{be} - K_{pc} - K_{pd} - K_{pe})\,.$$

Ignoring exchange between metal and porphin electrons

$$\Delta E(^5B_{2g} \to {}^5E_u) = w(e_g) - w(p) + 1.19\ \text{eV}\,.$$

The four suggested transitions are thus estimated at 1.6 and 1.8 eV and 2.2 and 2.6 eV. These transitions might again be expected to mix. This estimation places these bands of (x,y) polarization in the visible and near red region of the spectrum and could conceivably do considerably damage to the porphin spectrum in that region. The $a_{2u}(\pi) \to a_{1g}(d_{z^2})$ transition is estimated by

$$\begin{aligned}\Delta E(^5B_{2g} \to {}^5B_{1u}) &\approx w(a_{1g}) - w(a_{2u}) + \tfrac{2}{3}(K_{cd} + K_{bd} + K_{de} - K_{pc} - K_{pb} - K_{pe}) \\ &\approx w(a_{1g}) - w(a_{2u}) + 1.12\ \text{eV}\end{aligned}$$

and is sensitive to the environment of the central iron atom. From the $a_{2u}(\pi)$ this transition could lie anywhere from 1.6 – 2.4 eV; from the $a'_{2u}(\pi)$, 2.7 – 3.5 eV. The $b_{2u}(\pi) \to b_{1g}(d_{x^2-y^2})$ transition energy,

$$\begin{aligned}(^5B_{2g} \to {}^5B_{1u}) &\approx w(b_{2u}) - w(b_{1g}) + \tfrac{2}{3}(K_{ce} + K_{be} + K_{de} - K_{pc} - K_{pb} - K_{pd}) \approx \\ &\approx w(b_{2u}) - w(b_{1g}) + 1.39\ \text{eV}\,,\end{aligned}$$

is estimated at 4.6 in "non-planar" complexes and 5.4 eV in planar ones.

High spin ferric complexes have $^6A_{1g}$ ground states. Transitions from porphin π to $e_g(d_\pi)$ orbitals are estimated by

$$\Delta E(^6A_{1g} \rightarrow {}^6E_u) \approx w(e_g) - w(p) + \tfrac{3}{5}\,(K_{ab} + K_{bc} + K_{bd} + K_{be} - K_{pa} - K_{pc} - K_{pd} - K_{pe}) \approx w(e_g) - w(p) + 1.47\ \text{eV}\,,$$

giving transition energies averaging 1.9, 2.3, 2.6 and 3.0 eV for the high spin ferric complexes investigated. The two $a_{2u}(\pi) \rightarrow a_{1g}(d_{z^2})$ transitions are given by

$$\Delta E(^6A_{1g} \rightarrow {}^6A_{2u}) \approx w(a_{1g}) - w(a_{2u}) + \tfrac{3}{5}\,(K_{ad} + K_{cd} + K_{bd} + K_{de} - K_{pa} - K_{pb} - K_{pc} - K_{pe}) \approx w(a_{1g}) - w(a^2{}_u) + 1.47\ \text{eV}$$

and are estimated at 2.7 and 3.7 eV. The $b_{2u}(\pi) \rightarrow b_{1g}(d_{x^2-y^2})$ transition,

$$\Delta E(^6A_{1g} \rightarrow {}^6A_{2u}) = w(b_{2u}) - w(b_{1g}) + \tfrac{3}{5}\,(K_{ae} + K_{be} + K_{ce} + K_{de} - K_{ap} - K_{bp} - K_{cp} - K_{dp}) \approx w(b_{2u}) - w(b_{1g}) + 1.47\ \text{eV}\,,$$

is estimated at 4.6 eV.

The porphin to metal charge transfer transitions predicted by this model are summarized in Tab. 9.

Table 9. *Porphin π to Metal Change Transfer Transitions* (eV)

Transition	Polarization (D_{4h})	Low Spin		High Spin	
		Fe(II)[a]	Fe(III)CN[b]	Fe(II)[a]	Fe(III)OH[b]
$a_{2u}(\pi) \rightarrow e_g(d_\pi)$	x, y	—	0.2	1.6	1.9
$a_{1u}(\pi) \rightarrow e_g(d_\pi)$	x, y	—	0.5	1.8	2.2
$b_{1u}(\pi) \rightarrow e_g(d_\pi)$	x, y	—	1.0	2.2	2.6
$a'_{2u}(\pi) \rightarrow e_g(d_\pi)$	$x\,y$	—	1.3	2.6	3.0
$a_{2u}(\pi) \rightarrow a_{1g}(d_{z^2})$	z	1.2—1.7	1.5, 2.4	1.6—2.4	2.7
$a'_{2u}(\pi) \rightarrow a_{1g}(d_{z^2})$	z	2.4—2.9	2.6, 3.5	2.7—3.5	3.7
$b_{2u}(\pi) \rightarrow b_{1g}(d_{x^2-y^2})$	z	3.2—4.0	2.8, 4.1	4.6—5.4	4.6

[a] The ranges are for the various ligands and geometry of iron atom, which respectively affect the energy of a_{1g} (d_{z^2}) and b_{1g} ($d_{x^2-y^2}$).

[b] The two values for Fe(III)CN are for the two possible doublets.

In addition to the porphin to metal transitions just discussed, these calculations clearly demonstrate other charge transfer possibilities that might be quite important. We will examine especially the ferrous carbonyl and coplanar O_2 complexes where such transition possibilities are truly striking.

The MO scheme obtained for CO ferroporphin is summarized in Fig. 5 and demonstrates one of the only cases (the other is found in N_2) in which unoccupied orbitals other than the $b_{1g}(d_{x^2-y^2})$ of iron are calculated to lie between the porphin $e_g^*(\pi)$ and $b_{1u}(\pi)$. These new orbitals are principally composed of the $1\pi_g$ diatomic MO's of CO strongly antibonded to the $3d_\pi$'s of Fe. The principal ligand field $e_g(d_\pi)$ MO's, in turn, are strongly bonded to the CO $1\pi_g$ MO's as pictured in Fig. 4a. Transitions between these orbitals have an estimated dipole of 1.3 Å along the Fe–CO axis (Z), the largest calculated transition moment for any transition except that estimated for the Soret. The estimated transition energy is 2.8 eV + K, where K is the appropriate exchange integral. Approximating the exchange at 0.5 eV, as suggested by both the SCMO–PPP calculations and our $3d$-$3d$ values, this strong transition lies in the region of the experimental Soret band. The fact that the Soret band is so normal (see Fig. 8) in the CO complex, suggests that this band

must be further into the UV than calculated. Although about 50% of the bonding is destroyed by this transition, its high energy would seem to rule it out as the state responsible for the well-known photodissociation of the CO, for the latter has yields near unity with excitation at energies as low as 6600 Å [*51*].

A wealth of charge transfer possibilities arise from the results of the oxyferroporphin monohydrate calculations, summarized in Fig. 6. The O_2 $1\pi_g$ MO's, now split, one occupied and one empty, lie in the region between the top filled and lowest empty porphin orbitals. Foremost among the charge transfer possibilities is the transition between a MO composed principly of Fe $3d_{xz}$ and its unoccupied antibonding partner, principally O_2 $1\pi_g(Z)$. The estimated transition moment is 0.5 Å along Z. The suggested excited singlet is estimated to lie above the ground state by about 2.0 eV + K. A reasonable choice of the appropriate exchange integral places the corresponding transition in the visible. We have, at present, no evidence for such a band. However, this transition should be highly sensitive to the detailed bonding of the O_2 molecule. Placement of the O_2 molecule further from the iron atom, or deviations from pure coplanarity, as, for example, some compromise between coaxial and coplanar, would be expected to sizeably reduce both the transition energy and the large transition dipole. Geometries of this second type are certainly suggested from the results of the X-ray studies of ferrihaemoglobin azide [*70*]. A second predicted charge transfer state is the x polarized porphin $a_{2u}(\pi) \rightarrow O_2$ $1\pi_g(Z)$, calculated at 1.4 eV + K, where K in this case should be small. There are many other possibilities as a glance at Fig. 6 would suggest, but, since the two transitions discussed are estimated to have the largest transition dipoles it is hard to conceive of their absence in the spectrum in favor of other less probable transitions.

Before concluding this discussion we should emphasize that the energies predicted for these charge transfer states are particularly sensitive to certain deficiencies in the present model. These are, in particular: (i) the fitting of $\varkappa$ to $\pi \rightarrow \pi^*$ transitions giving a value that may not be so good for other transitions; (ii) the sensitivity of charge transfer transitions to the geometry, which we have often had to assume; and (iii) the sensitivity of these transitions to the relative spacing of the d and π orbitals which traces back to the H_{pp} used for iron, which are based on extrapolation. Nonetheless the catalogue of possible transitions should be useful for experimentalists whose identification of bands will be necessary for testing and refining the present model.

4. $d \rightarrow d$ Transitions

A number of $3d \rightarrow 3d$ ligand field transitions are possible in these complexes. Strictly speaking, in D_{4h} symmetry all are $g \rightarrow g$ forbidden. To the extent that these molecular systems undergo C_{4v} or C_{2v} distortion, such as is introduced by the non-planarity of the iron atom or by additional fifth and sixth position ligands, some of these transitions will gain intensity. Considering a reduction of symmetry to C_{2v} the orbital symmetries are $a_2(d_{xy})$; $b_1(d_{xz})$; $b_2(d_{yz})$; $a_1(d_{z^2})$; $a_1(d_{x^2-y^2})$. Transitions $a_1 \leftrightarrow (b_1, b_2)$ and $a_2 \leftrightarrow (b_2, b_1)$ are, respectively, (x, y) polarized. Transitions $a_1 \leftrightarrow a_1$ are z polarized. Other transitions remain forbidden.

Using the model previously developed for estimating transition energies

Table 10. *Allowed $d \rightarrow d$ Transitions Under C_{2v} Distortion* (eV)

Transition	Ferric, $S = \frac{1}{2}$	Ferrous, $S = 2$	Ferrous, $S = 0$
$d_{xy} \rightarrow d_\pi$	$^2E_g \rightarrow {}^2B_{2g}$ 0.1	$^5B_{2g} \rightarrow {}^5E_g$ 0.1	
$d_\pi \rightarrow d_{z^2}$	$^2E_g \rightarrow {}^2B_{2g}$ 2.3 $^2B'_{2g}$ 1.9 $^2A_{1g}$ 3.6 $^2B_{1g}$ 2.2		$^1A_{1g} \rightarrow {}^1E_g$ 1.0—1.9
$d_\pi \rightarrow d_{x^2-y^2}$	$^2E_g \rightarrow {}^2A_{2g} < 2.9$ $^2A'_{2g} < 2.5$ $^2B_{1g} < 4.2$ $^2A_{1g} < 2.8$		$^1A_{1g} \rightarrow {}^1E_g$ planar 3.3 non-planar 2.6

$b, c \rightarrow d, e$ (recall the correspondence $a = d_{xy}$, $b = d_{yz}$, $c = d_{xz}$, $d = d_{z^2}$, $e = d_{x^2-y^2}$) in the low spin ferrous complexes are given by*

$$^1E_B(c \rightarrow d) - {}^1E_A \approx w(d) - w(c) + K_{dc} \approx w(d) - w(c) + 0.46\ (0.66)\ \text{eV}\ .$$

In the high spin ferrous case the transitions $a \rightarrow b$, c are given by

$$^5E_D(a \rightarrow b) - {}^5E_D \approx w(b) - w(a) + \tfrac{2}{3}\,(K_{bc} + K_{bd} + K_{be} - K_{ac} - K_{ad} - K_{ae}) \approx w(b) - w(a)\ .$$

All $d \rightarrow d$ transitions in high spin ferric are spin forbidden. In low spin ferric complexes allowed transitions $b, c \rightarrow d, e$ are estimated by

$$^2E_B(b \rightarrow d) - {}^2E_A \approx w(d) - w(b) - \tfrac{1}{6}\,(K_{db} + K_{dc}) + \tfrac{4}{3}\,K_{bc} \approx w(d) - w(b) + 0.73\ (0.66)\ \text{eV}\ .$$

$$^2E'_B(b \rightarrow d) - {}^2E_A \approx w(d) + \tfrac{5}{6}\,(K_{db} + K_{dc}) - \tfrac{2}{3}\,K_{bc} \approx w(d) - w(b) + 0.33\ (0.66)\ \text{eV}\ .$$

$$^2E_C(b \rightarrow d) - {}^2E_A \approx w(d) - w(c) + 3K_{bc} \approx w(d) - w(c) + 1.98\ \text{eV}\ .$$

$$^2E'_C(b \rightarrow d) - {}^2E_A \approx w(d) - w(c) + K_{bc} \approx w(d) - w(c) + 0.66\ \text{eV}\ ,$$

where we have taken $W_C = W_B + 2\,K_{bc}$ as described previously.

A summary of the spin allowed transitions and their transition energies, estimated from these equations, is given in Tab. 10. Transitions involving the $a_1(d_{x^2-y^2})$ ligand field orbital will be sensitive to the geometry of the iron atom relative to the porphin plane. Transitions to the $a_1(d_{z^2})$ ligand field orbital will be sensitive to the presence of fifth and sixth coordinating ligands. Transitions involving the $3d_\pi$ ligand field orbitals may be split depending on the amount of C_{2v} distortion. Judging from our ferrous hydrate calculations this split might be $\sim$500 cm^{-1}; from GRIFFITH's [*29*] conclusions on ferrihaemoglobin azide, 600—1500 cm^{-1}. If resolved in careful absorption spectrum, this predicted splitting might provide some guide in the location of transitions to and from the $3d_\pi$'s.

The transition $e_g(d_\pi) \rightarrow a_{1g}(d_{z^2})$ supplies a very plausible pathway for the well-known photodissociation of ferrous porphyrin complexes with CO and CN$^-$ [*51, 40*]. Tab. 10 shows that this transition is at fairly low energy and in the C_{4v} point group has the same symmetry as the allowed $a_{2u}(\pi) \rightarrow e_g^*(\pi)$, from which it could

* In this and the following expressions the value in parenthesis is used when orbital e replaces d.

be produced by radiationless transition. Since the $e_g(d_\pi)$ contributes to the bonding of CO to iron while $a_{1g}(d_{z^2})$ is antibonding the CO will start to dissociate. Fig. 5 suggests that the reaction would run down-hill producing an iron-porphyrin in an $S = 1$ state and ground state CO. (That this reaction apparently does not go in ferric cyanide complexes might stem from several factors: The existence of an odd electron should greatly alter various radiationless transition rates and the final products, being ions, may not easily separate.)

5. *Interpretation of Iron Porphyrin Spectra*

(i) Low spin cases: As stated above the low spin ferrous complexes except for O_2 have completely normal spectra. That this is so undoubtedly stems from the fact the d_π orbitals are filled. As shown in Tab. 9 any charge transfer transitions are z polarized and are probably quite distinct from the $\pi \rightarrow \pi^*$ spectra, which remain undisturbed. The transitions $e_g(d_\pi) \rightarrow a_{1g}(d_{z^2})$ should stand in the near infrared in a region of the spectrum that has no competing absorption and is a good $d \rightarrow d$ transition to seek experimentally.

The 900 mμ band unique to the O_2 ferrous complex can be attributed either to the z polarized $b_1(d_{xz}) \rightarrow O_2\ 1\pi_g(Z)$ or to the x polarized $a_{2u}(\pi) \rightarrow O_2\ 1\pi_g(Z)$. Studies on the polarization of this band will help determine its nature.

The ferric low spin complexes also show a more or less "normal" spectrum. In addition to the transitions possible in ferrous low spin, as shown in Tab. 9, these compounds should have some low energy charge transfer absorptions $a_{2u}(\pi)$, $a_{1u}(\pi)$, $b_{1u}(\pi)$, $a'_{2u}(\pi) \rightarrow e_g(d_\pi)$ that are x, y polarized.

(ii) High spin cases: Neither high spin ferrous nor ferric are "normal" in the visible region. The ferric complexes possess two extra bands and the ferrous probably at least one. As shown in Tab. 9, the (x, y) polarized charge transfer transitions that are predicted to lie between 0.2 and 1.3 eV in ferric low spin are predicted between 1.6 and 2.6 eV in ferrous high spin and between 1.9 and 3.0 in ferric high spin. It would seem reasonable to suppose that the extra bands in the near infrared and visible are attributable to these (x, y) polarized charge transfer transitions and that the higher energy pair $a'_{2u}(\pi)$, $b_{1u}(\pi) \rightarrow e_g(d_\pi)$ perturb the visible region and the lower energy pair $a_{1u}(\pi)$, $a_{2u}(\pi) \rightarrow e_g(d_\pi)$ are responsible for the bands observed in the near infrared [*22*]. That these charge transfer transitions should heavily mix with the $\pi \rightarrow \pi^*$ transitions is not surprising since the $e_g(d_\pi)$ orbitals have considerable porphin π character, and in the high spin ferric complexes these orbitals are 35—45% porphin π.

(iii) Alternative Interpretations: Although the charge transfer interpretation for the extra bands in the high spin case suggested by BRILL and WILLIAMS [*6*], is supported by the present calculations, it is useful to keep alternative interpretations in mind. SCHELER, SCHOFFA, and JUNG [*66*] have pointed out that the strong correspondence between the four banded ferric high spin spectra and the four banded free base spectrum shown in Fig. 10. SCHELER [*65*] has suggested various complexing situations around the central metal that might bring about this "pseudo free base" spectrum.

Another possible cause of extra bands exists in the iron compounds with non-zero spin. In the simplest case of a ground state doublet due to an odd d electron, the $\pi \rightarrow \pi^*$ excitation that normally gives a singlet and a triplet gives

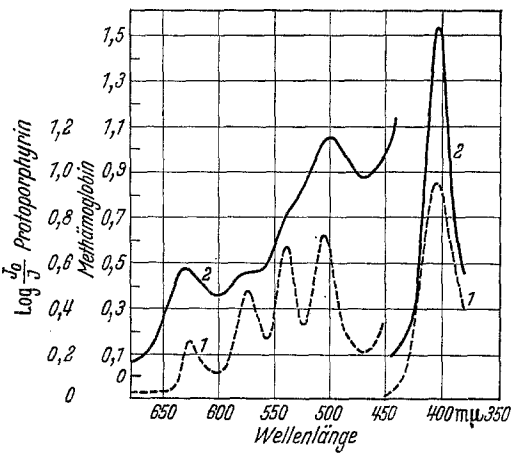

Fig. 10. Comparison of the absorption spectra of neutral free base protoporphyrin (curve 1) and acid metmyoglobin (ferric-high spin) (curve 2) [66]

two doublets and a quartet [26]. One doublet corresponds to the normal excited singlet and one to the normal triplet. The latter borrows intensity due to exchange interaction between the π and d electrons. Similar, but more complex situations, arise when the ground state has a higher spin. In iron the d electrons can be quite delocalized and so exchange interactions might be sizeable. Whether or not this paramagnetic enhancement of the $\pi \rightarrow \pi^*$ triplet excitation should be significant is currently under theoretical investigation in our laboratory.

6. *Soft X-Ray Spectrum*

Böke in 1957 [5] examined the soft X-ray spectrum of haemin in water. This spectrum appears as Fig. 11. Three peaks are clearly discernable lying at 11, 15.5 and 23.5 V from the K absorption onset. The two major peaks were assigned to transitions from the Fe $1s$ to $4p$ orbitals, the degeneracy of which is split by the ligand field established by porphin [13]. The lesser peak, at 11 V, was hypothesized to represent transitions from $1s$ to $4s$ or $3d$ [14]. The present calculations which include the $3d$, $4s$ and $4p$ orbitals of Fe explicitly might be used to examine this spectrum.

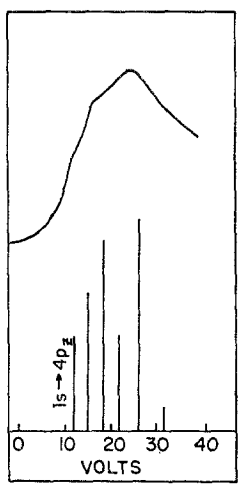

Fig. 11. Soft X-Ray Spectrum of Haemin (Ferrihaemoglobin Chloride); spectrum [5]

The $4p$ ligand field is, of course, sensitive to the location of the iron atom relative to the porphin plane, and to the location of fifth and sixth position coordinating ligands. Examining the ferric chloride calculation, the principal $a_{2u}(4p_z)$ orbital is almost pure Fe $4p_z$. The $4p_x$ and $4p_y$ orbitals, on the other hand, are mixed heavily into several MO's of $e_u(\sigma)$ symmetry. Estimating the intensity of $1s \rightarrow 4p$ transitions by the appropriate coefficients in the several MO's with large $4p$ character, we have created under Böke's spectrum the spectrum predicted

by this model. The origin is, of course, somewhat arbitrary as we have not explicitly considered the Fe $1s$ functions, and we have simply added 7 V to each MO energy to give the most suggestive plot.

Two points are especially worthy of note. First, at least three bands of high intensity are predicted for $1s \rightarrow 4p$ transitions, and one need not postulate $1s \rightarrow 4s$ and $1s \rightarrow 3d$ atomic transitions, formally forbidden, to explain the observed three peaks. The second point is that the calculated energy differences between the three most intense lines corresponds fairly well to the energy differences between the observed peaks. If, indeed, Böke's peaks correspond to $1s \rightarrow 4p$ transitions, then the second point is rather important as a verification of our method for choosing $4p$ exponential constants, the value of which greatly determines the $4p$ ligand field.

e) Electronic Population

The net charges of the various iron porphyrin complexes have been discussed individually in earlier sections and a brief summary is in order. We find that the high spin has a net charge $+0.05$ greater than the low spin for both ferrous and ferric iron. Further ferric has on the average $+0.05$ greater charge than ferrous. Thus the distinction between ferrous and ferric is not so much in net charge but in d orbital occupancy, which is $(d)^6$ and $(d)^5$ respectively. An exception to these net charges is coplanar oxyferroporphin hydrate, which has a greater positive charge than any other complex examined, including those formally ferric. However, in this case the large calculated covalency of the d_{xz} orbital (see Tab. 5) might lead us to consider this compound to be $(d)^4$ and hence the iron atom to be tetravalent.

Although net charge is not at present directly measurable, the s orbital population and p and d orbital anisotropy can be explored by Mössbauer spectroscopy. Our calculations show that the net population of $4s$ has a spin dependence in ferrous complexes, where it is greater with high spin. In ferric complexes the $4s$ population is dependent not on spin but on iron to counter-ion bond distance.

Some of the results of a Mössbauer investigation by LANG and MARSHALL appear in Tab. 11 [*45*]. It is seen that the chemical shifts for ferrous haemoglobins are spin dependent in a way which would be in agreement with our calculated $4s$ populations. The calculated $4s$ population in the carbonyl complex is not in agreement with these results. However, as with the ferric complexes, this $4s$ electronic population is dependent on the length of the bond between iron and the fifth position ligand.

With the Mössbauer data available we can examine some of the detailed electronic structure of the $3d$ and $4p$ metal orbitals [*2, 1*]. It is not our purpose here to examine the observed quadrupole splittings in great detail, but only the general features which they might reflect.

Low spin ferrous complexes should have, to a first approximation, no quadrupole splitting. That the carbonyl complex has some small splitting is attributed to the anisotropic covalency of the d and p orbitals. An examination of the total electronic populations of the $3d$ orbitals for this complex, Case XII of Tab. 6, demonstrates these anisotropies. The numbers to compare are the total populations of the three lowest $3d$ orbitals, $3d_{xy}$, $3d_{yz}$ and $3d_{xz}$, with one another, the total populations of the two higher $3d$ orbitals, $3d_{x^2-y^2}$ and $3d_{z^2}$ with one another,

Table 11. *Mössbauer Results, From* LANG *and* MARSHALL, [45]

Material[a]	Temperature	Quadrupole[b] Splitting	Shift[b]	S
HiCN	195 °K	1.39	0.17	1/2
HiN_3	195 °K	2.30	0.15	1/2
HiOH	195 °K	1.57	0.18	5/2 – 1/2
HiOH	77 °K	1.9	0.2	5/2 – 1/2
HiH_2O	195 °K	2.00	0.20	5/2
HbO_2	195 °K	1.89	0.20	0
HbO_2	77 °K	2.19	0.26	0
HbO_2	1.2 °K	2.24	0.24	0
Hb	195 °K	2.40	0.90	2
Hb	4 °K	2.40	0.91	2
HbCO	195 °K	0.36	0.18	0
HbCO	4 °K	0.36	0.26	0

[a] Hi = ferric haemoglobin,
Hb = ferrous.
[b] Units are mm/sec. The authors' estimated error is ±0.05 mm/sec.

and the total population of the three $4p$ orbitals. Each subgroup, if evenly occupied, would demonstrated no first order deviations from cubic symmetry. We notice in the low spin carbonyl complex most of the calculated asymmetry appears in the formally filled lower three d orbitals and in the $4p$ orbitals. In the cases of low spin ferrous hydrates the asymmetry is mostly in the formally unoccupied $3d_{x^2-y^2}$ and $3d_{z^2}$. Oxyhaemoglobin shows a large quadrupole splitting, consistent with the great degree of covalency and anisotropy which we calculate. The subtle distinction between ferrous and ferric which we have noted for this complex is also commented on by LANG and MARSHALL in the analysis of their data.

In the absence of covalency ferric low spin complexes should have a quadrupole splitting comparible to ferrous high spin; in the former case there is one hole in the three lower orbitals whose complete occupancy would establish cubic symmetry (as in ferrous low spin), in the latter case there is one additional electron beyond the spherically symmetric half filled $3d$ subshell. That the ferric low spin value is found somewhat lower correlates well with the anisotropies indicated in Tab. 6. High spin ferric should demonstrate no quadrupole splitting. The surprisingly large value observed for methaemoglobin hydroxide can, perhaps, be explained by the surprisingly large covalency found for the $3d_\pi$ orbitals (Tab. 5). The anisotropy resulting from this covalency is clearly demonstrated in Tab. 6.

The correspondence between anisotropic electronic population and the quadrupole splitting is reasonable. There are so many factors entering into the theoretical calculation of this splitting, however, that a consideration of covalency alone must be regarded with some care.

There is one additional point that bears special attention. The porphin orbitals, the iron orbitals, and even the *trends* in the net charges are not sensitive to the atomic orbital ionization potentials of Fe which we have chosen to average and use for the diagonal terms of the energy matrix. However, the relation of the ligand field orbitals to those of porphin, and the calculated net charge on the iron atom is sensitive to the relative values of these H_{pp}.

A plot of chemical half cell potential versus calculated net charge on the central metal atom appears in Fig. 12 for all the metals which we have yet considered. It would be reasonable to suppose that the chemical half cell potential reflects in some intrinsic way the ability of a metal to lose electrons. This ability to lose electrons also determines the net metal charge in a porphyrin complex. The failure of Fe and Mn to fit in this pattern could mean perhaps a failure on our part to parametrize these cases properly and that a better treatment would bring these metals into line. The results for a different H_{pp} calculated from atomic data in another "reasonable" way are shown in Fig. 13. Another interpretation is that indeed these metals are exceptions: In their porphyrin complexes they have

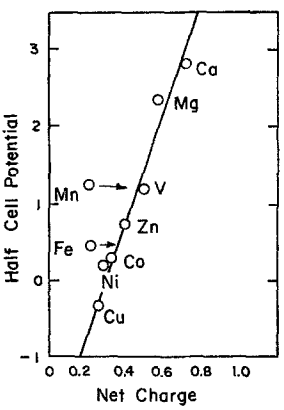

Fig. 12

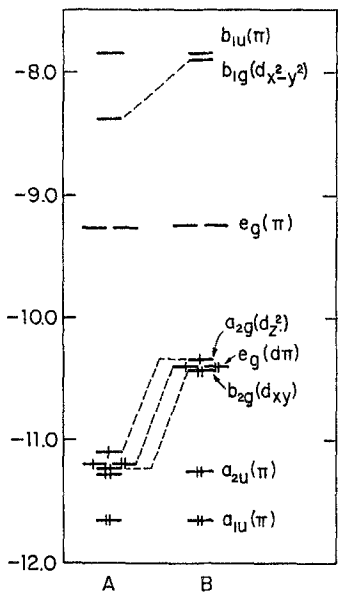

Fig. 13

Fig. 12. Calculated Metal Net Charge *vs* Half Cell Potential. All half cell potentials are for $M \rightarrow M^{++} + 2e$. Arrows indicate the change in net charge calculated on Mn and Fe by assuming a different model for obtaining appropriate ionization processes; see text

Fig. 13. Dependence of Iron 3*d* Manifold on H_{pp} for planar ferrous porphin. A assumes a d^6s^2 ground state of iron; B assumes d^7s ground configuration of iron

built up far less net charge than they "should" according to a more intrinsic measure of electronegativity. This peculiarity, in turn, could relate to the role of these complexes in oxidationreduction. Future investigations, both theoretical and experimental, will be needed to explore this relation.

Discussion

a) Origin of the ligand field

The present paper represents an attempt to understand the *d* electronic structure of iron porphyrins within a single theoretical model that comprehends a great many other spectroscopic, magnetic, and chemical facts. However, it may be useful here to relate the present theory to previous theoretical consideration given to the *d* electrons.

PAULING and CORYELL [57], in their first classic paper on the magnetic properties of haem compounds, gave the first theoretical discussion. They pointed out

that in a square planar complex the metal should form dsp^2 hybrids and in an octahedral complex d^2sp^3. The former implies intermediate spin and the latter low spin. To account for high spin they postulated that the complexes were "ionic". However, the reason certain complexes should be ionic and others covalent was not specified.

More modern theory has worked with the crystal field model [*28, 43, 56, 50, 32*]. This approach parametrizes the splitting of the d orbitals by the porphyrin-ligand system and goes on to consider multiplet structure and other parameters assuming the iron d orbitals are atomic. The fact that the iron porphyrin complexes are either high or low spin is accounted for by assuming that the field is basically octahedral and that the energy gap Δ between the $d_\gamma(d_{xy}, d_{yz}, d_{xz})$ and the $d_\varepsilon(d_{z^2}, d_{x^2-y^2})$ orbitals is small in high spin or large in low spin complexes [*44, 56*]. The fifth and sixth ligands are assumed to affect Δ so that H_2O, OH^-, F^-, for example, give high spin and CO, CN^- low spin.

The extended Hückel model used in this study gives results that can be related back to both older theories but adds a new dimension to the problem. Planar iron porphin with no extra ligands* is predicted to be intermediate spin with the orbitals d_{xy}, d_{yz}, d_{xz}, d_{z^2} close in energy and $d_{x^2-y^2}$ much higher, a result parallel to that for dsp^2 bonding. The addition of a fifth weak ligand raises d_{z^2} just enough to bring about low spin, i.e., the equivalent of d^2sp^3 hybridization. The calculations go on to state unambiguously that high spin complexes necessarily mean the iron atom is out of plane. Only in this geometry can fifth and sixth ligands so influence Δ as to give rise to only high and low spin ground states. In the present model, it is the combination of weak ligand and non-planar geometry that gives rise to the high spin complex, the so-called "ionic" complex. However, as shown in Tab. 7, the high spin complex is calculated to be only ~0.05 more ionic than low spin.

Since the present model differentiates strong and weak field ligands with good reliability, a few qualitative remarks are, perhaps, in order. We can find three factors in this model mainly responsible for establishing the ligand field. First, and most obvious, the distance between the iron atom and the chelating atom of the ligand group is paramount in determining its effect on the resulting ligand field [*38*]. A water molecule 2.1 Å from the iron atom in ferrous porphin has a marked affect on the ligand field established; a water molecule 2.6 Å is hardly felt. A second reason, and somewhat related to the first, is the "size" of the atomic orbitals centered on the chelating atom. Expanded orbitals, with small exponential constants, lead directly to larger interactions. This effect would, by itself, establish the order C > N > O > F were it not for the fact that these atoms in molecules build up negative charges in the reverse of this order, and a proper treatment might be expected to increase the orbital size with net negative charge**. Third, and seemingly most important in establishing the ligand field, is the availability of ligand orbitals of nearly equal energies to those of the metal 3*d*'s with which they can combine. If ligand orbitals of the proper symmetry appear above the metal 3*d*'s, they depress those with which they bond; if they appear below they raise those with which they antibond. The orbitals of fluorine are low in energy, and do not greatly disturb the ligand field established by porphin. The filled $2p_\pi$ orbitals of OH^- are higher in energy, raising the $e_g(d_\pi)$ orbitals in

* Since attempts to isolate ferrous porphyrins free from addition ligands have not proved successful [*71*], the compound may or may not be planar.

** A truly self-consistent charge procedure might be expected to adjust not only the energy matrix to reflect the net atomic charge but also the exponential constants of the basis set. This, however, would necessitate the recalculation of orbital overlap with each iteration greatly expanding the computation time. Fortunately the charge build-up is generally small except for fluorine. The fluoride calculation is therefore less reliable.

the ferric hydroxide complex. O_2 has two partially filled $1\pi_g$ MO's which strongly interact. CO and CN have filled σ levels near enough in orbital energy to that of the $3d_{z^2}$ to raise its energy greatly; in some cases the empty $1\pi_g$ orbitals of these ligands lower the $3d_\pi$'s, further increasing the strength of the ligand field. This effect can be measured somewhat by the differences in the net charges of the iron atom and the chelating atom. For the ligands we have considered, a large negative charge on the chelating atom generally indicates that the perturbing occupied orbitals lie considerably below the $3d$ orbitals. Again the order established is C > N > O > F as observed; the exception being paramagnetic O_2.

b) Summary of Results: Biological Implications

X-ray [*37*] and magnetic susceptibility investigators [*49*] have previously suggested that spin state and iron non-planarity might be related. A principal result of the present study is to claim, and this is presently rather a prediction, that high spin iron is necessarily out-of-plane. Therefore, insofar as a protein can constrain geometry changes, it can affect spin state and hence other properties of the iron porphyrin. GRIFFITH [*28*] had previously shown that the diamagnetism of the oxyhemoglobin complex shows that the O_2 is not perpendicular to the haem plane. The present calculations show that such a geometry implies immediate oxidation. Hence there is a need for the porphyrin to sit in a crevice in the protein and not on the surface. The model also shows why, unique among ferrous low spin complexes, the O_2 shows bands in the near infrared.

Three further results are also of interest. Although N_2 complexes with iron porphyrins have been suspected of playing a role in nigrogen fixation [*18*], the present calculations suggest that an N_2 complex with ferrous porphyrin is unstable. The model also suggests that the photodissociation of ferrous complexes with CO passes through the excited state $e_g(d_\pi) \rightarrow a_{1g}(d_{z^2})$, which is also the $d \rightarrow d$ transition most likely to be observable. Finally the model spells out in far more detail than was previously possible [*6*, *54*] the charge transfer transitions responsible for the extra bands in the high spin iron complexes.

Acknowledgements. This research was supported in part by Public Health Service Research Grant G.M. 10833, from the Division of General Medical Sciences. The numerical work was done at the Computing center of Harvard University, which provided the necessary technical assistance. Finally we wish to thank GEORGE LANG and WILLIAM MARSHALL for their Mössbauer results, RICHARD FRANKEL for his excellent spectra of haem complexes, and ROBERT AKE, PETER OFFENHARTZ, and DAN URRY for more than useful discussions.

References

[*1*] BEARDEN, A. J., and T. H. MOSS: Non-Hemeiron proteins. SAN PIETRO, A., Ed. Yellow Springs. Ohio: The Antioch Press 1965.
[*2*] — —, W. S. CAUGHEY, and C. A. BEAUDREAU: Proc. Natl. Acad. Sci. (U.S.) **53**, 1246 (1965).
[*3*] BECKER, R. S., and J. B. ALLISON: J. physic. Chem. **67**, 2662, 2675 (1963).
[*4*] BERTHIER, G., P. MILLIE, and A. VEILLARD: J. Chim. physique **62**, 20 (1965).
[*5*] BÖKE, K.: Z. physik. Chemie (Frankf.) **11**, 326 (1957).
[*6*] BRILL, A. S., and R. J. P. WILLIAMS: Biochem. J. **78**, 259 (1961).
[*7*] BROCKWAY, L. O., and J. S. ANDERSON: Trans. Faraday Soc. **33**, 1233 (1937).
[*8*] CALVIN, M.: Rev. Pure Appl. Chem. **15**, 1 (1965).
[*9*] CAUGHEY, W. S., R. M. DEAL, C. WEISS, and M. GOUTERMAN: J. Mol. Spectroskopy. **16**, 451 (1965).
[*10*] CLEMENTI, E.: J. chem. Physics **41**, 303 (1964).
[*11*] —, and D. L. RAIMONDI: J. chem. Physics **38**, 2686 (1963).

[12] CONDON, E. U., and G. H. SHORTLEY: The theory of atomic spectra, Chpt. 7: Cambridge: University Press 1951.
[13] COTTON, F. A., and C. J. BALLHAUSEN: J. chem. Physics **25**, 617 (1956).
[14] —, and H. P. HANSON: J. chem. Physics **26**, 1758 (1957).
[15] DOROUGH, G. D., J. R. MILLER, and F. M. HUENNEKENS: J. Am. chem. Soc. **73**, 4315 (1951).
[16] DRABKIN, D. L.: Haematin enzymes, p. 142—168. FALK, J. E., R. LEMBERG, and R. K. MORTON, Ed. Oxford: Pergamon Press 1961.
[17] Paper VII: EASTWOOD, D., L. EDWARDS, M. GOUTERMAN, and J. STEINFELD: J. mol. Spectroskopy (In press).
[18] ELLFOLK, N.: Acta chem. Scand. **15**, 975 (1961).
[19] ESTABROOK, R. W.: Haematin enzymes, p. 436—456, FALK, J. E., R. LEMBERG, and R. K. MORTON, Ed. Oxford: Pergamon Press 1961.
[20] FLEISCHER, E. B., C. K. MILLER, and L. E. WEBB: J. Am. chem. Soc. **86**, 2342 (1964).
[21] FRANKEL, R.: Unpublished spectra.
[22] GEORGE, P., J. BEETLESTONE, and J. S. GRIFFITH: Haematin enzymes, p. 105—141. FALK, J. E., R. LEMBERG, and R. K. MORTON, Ed. Oxford: Pergamon Press 1961.
[23] GIBSON, J. F., and D. J. E. INGRAM: Nature **180**, 29 (1957).
[24] GONSER, U., and R. W. GRANT: Biophys. J. **5**, 823 (1965).
[25] GOUTERMAN, M.: J. chem. Physics **30**, 1139 (1959).
[26] Paper I: GOUTERMAN, M.: J. mol. Spectroskopy **6**, 138 (1961).
[27] Paper II: GOUTERMAN, M., G. H. WAGNIERE, and L. C. SNYDER: J. mol. Spectroskopy, **11**, 108 (1963).
[28] GRIFFITH, J. S.: Proc. Roy. Soc. (Lond.) **235A**, 23 (1956).
[29] — Nature **180**, 29 (1957).
[30] HAMOR, T. A., W. S. CAUGHEY, and J. L. HOARD: J. Am. chem. Soc. **87**, 2305 (1965).
[31] HANANIA, G. I. H., A. YEGHIAYAN, and B. F. CAMERON: Biochem. J. **98**, 189 (1966).
[32] HARRIS, G. M.: Theoret. chim. Acta **5**, 379 (1966).
[33] HARTREE, E. F.: Ann. Repts. Prog. Chem. **43**, 287 (1946).
[34] HERZBERG, G.: Spectra of diatomic molecules, Appendices. Princeton, N.J.: D. Van Nostrand 1950.
[35] HINZE, J., and H. H. JAFFÉ: Can. J. Chem. **41**, 1315 (1963).
[36] HOARD, J. L., M. J. HAMOR, and T. A. HAMOR: J. Am. chem. Soc. **85**, 2334 (1963).
[37] — — —, and W. S. CAUGHEY: J. Am. chem. Soc. **87**, 2312 (1965).
[38] JORGENSEN, C. K.: Absorption spectra and chemical bonding in complexes. Oxford: Pergamon Press 1961.
[39] KEILIN, D., and E. F. HARTREE: Biochem. J. **49**, 88 (1951).
[40] — — Biochem. J. **61**, 153 (1955).
[41] KENDREW, J. C.: Science **139**, 1259 (1963).
[42] KOENIG, D. F.: Acta Cryst. **18**, 663 (1965).
[43] KOTANI, M.: Prog. Theoret. Phys. (Kyoto), supplement No. 17, p. 4 (1961).
[44] — Advan. chem. Physics **7**, 159 (1964).
[45] LANG, G., and W. MARSHALL: J. mol. Biol. **18**, 385 (1966).
[46] LEMBERG, R., and J. W. LEGGE: Hematin compounds and bile pigments, p. 748. New York: Interscience 1949.
[47] LEVER, A. P. B.: J. chem. Soc. (Lond.) **1965**, 1821.
[48] LOACH, P. A. and M. CALVIN: Biochemistry **2**, 361 (1963).
[49] LUMRY, R., A. SOLKAKKEN, J. SULLIVAN, and L. H. REYERSON: J. Am. chem. Soc. **84**, 142 (1962).
[50] MCCLURE, D. S.: Radiation research, Supplement **2**, 218 (1960).
[51] MCLAREN, A. D., and D. SHUGAR: Photochemistry of proteins and nucleic acids, p. 110. New York: Pergamon Press Book, The MacMillan Co. 1964.
[52] MULLIKEN, R. S.: J. Chim. physique **46**, 497, 673 (1949).
[53] — J. chem. Physics **23**, 1833, 1841 (1955).
[54] OFFENHARTZ, P. O'D.: J. chem. Physics **42**, 3566 (1965).
[55] OHNO, K., Y. TANABE, and F. SASAKI: Theoret. chim. Acta **1**, 378 (1962).

[56] ORGEL, L. E.: Haematin enzymes, p. 1—13, FALK, J. E., R. LEMBERG, and R. K. MORTON, Ed. Oxford: Pergamon Press 1961.
[57] PAULING, L., and C. D. CORYELL: Proc. Nat. Acad. Sci. (U.S.) **22**, 159, 210 (1936).
[58] —, and E. B. WILSON: Introduction to quantum mechanics, Chpt. 7. New York: McGraw-Hill 1935.
[59] PENFOLD, B. R., and J. A. GRIGOR: Acta Cryst. **12**, 850 (1959).
[60] PLATT, J. R.: Radiation biology, Vol. III, Chpt. 2. HOLLAENDER, A., Ed. New York: McGraw-Hill 1956.
[61] POWELL, H. M., and G. W. R. BARTINDALE: J. chem. Soc. (Lond.) **1945**, 799.
[62] PULLMAN, B., C. SPANJAARD, and G. BERTHIER: Proc. Natl. Acad. Sci. (U.S.) **46**, 1011 (1960).
[63] RACAH, G.: Phys. Rev. **62**, 438 (1942).
[64] ROOTHAAN, C. C. J.: Rev. mod. Phys. **23**, 69 (1951).
[65] SCHELER, W.: Biochem. Z. **332**, 344, 542 (1960).
[66] —, G. SCHOFFA, and F. JUNG: Biochem. Z. **329**, 232 (1957).
[67] SILVERS, S., and A. TULINSKY: J. Am. chem. Soc. **86**, 927 (1964).
[68] SKINNER, H. A., and F. H. SUMNER: J. inorg. nucl. Chem. **4**, 245 (1957).
[69] SLATER, J. C.: Quantum theory of atomic structure, Vol. I. App. 21; Vol. II, App. 21. New York: McGraw-Hill 1960.
[70] STRYER, L., J. C. KENDREW, and H. C. WATSON: J. mol. Biol. **8**, 96 (1964).
[71] URRY, D.: Proc. Natl. Acad. Sci. (U.S.) **54**, 640 (1965).
[72] WANG, J. H.: Oxygenases, Chapt. 11. HAYAISHI, O., Ed. New York: Academic Press 1962.
[73] WATSON, R. E.: Phys. Rev. **119**, 1934 (1960).
[74] Paper III: WEISS, C., H. KOBAYASHI, and M. GOUTERMAN: J. mol. Spectroskopy. **16**, 415 (1965).
[75] WOLFSBERG, M., and L. HELMHOLTZ: J. chem. Physics **20**, 837 (1952).
[76] ZERNER, M.: Ph. D. Thesis, Dept. of Chemistry, Harvard University (1966).
[77] Paper IV: ZERNER, M., and M. GOUTERMAN: Theoret. chim. Acta **4**, 44 (1966).
[78] Papers V and VI: ZERNER, M., and M. GOUTERMAN: Inorg. Chem. **5**, 1699, 1707 (1966).

Dr. HIROSHI KOBAYASHI
Department of Chemistry
Tokyo Institute of Technology
Meguro-ku, Tokyo, Japan

Professor MARTIN GOUTERMAN
Department of Chemistry
University of Washington
Seattle, Washington 98105